Spectral Reflectance Characteristics of Kimberlite Indicator Minerals and Other Selected Mineral Grains

Matthew McMahon, B.Sc.

Masters of Science in Earth Science

Submitted in partial fulfillment of the requirements for the degree of

Masters of Science

Department of Earth Sciences, Brock University

St. Catharines, Ontario

Abstract

High chromium content in kimberlite indicator minerals such as pyrope garnet and diopside is often correlated with the presence of diamonds. In this study, kimberlite indicator minerals were examined using visible light reflectance spectroscopy to determine if chromium content can be correlated with spectral absorption features. The depth of absorption features in the visible spectral region were correlated with the molecular percentage of chromium and other first series transition metal elements obtained by electron microprobe data. In the visible part of the spectrum, chromium is evident by 3 absorption features in the pyrope reflectance spectrum; one isolated and narrow feature at the wavelength 689 nm was used to correlate with the chromium mol %. The isolation of this feature in the pyrope spectra is advantageous since it is not directly affected by other proximal absorption bands that could be caused by other transition metals. Analysis of the feature indicates that as grain volume increases the depth of the absorption feature will also increase. Clustering grain volumes into fractions yields better correlation between absorption depth and mol % chromium.

Other types of garnet (almandine, grossular, spessartine) and kimberlite indicator minerals (olivine, diopside, chromite, ilmenite) were analyzed to determine if other absorption features could be used to predict the proportion of specific transition metal elements. Diopside in particular illustrates the same isolated chromium absorption feature as pyrope and may indicate mol percent but needs further study with larger sample sets.

Table of Contents

List of Tables and Figures

Chapter 2

Chapter 3

Chapter 4

Chapter 5

Acknowledgments

I would like to express my gratitude to my supervisor, Dr. Frank Fueten. The patience, advise, expertise and understanding contributed greatly to this project and my graduate experience. Without his motivation and encouragement I would not have considered a graduate career in Earth Science. He provided me with direction, technical support and became more of a mentor and friend, than a professor. I would also like to thank the other members of my committee, Paul Budkewitsch of Natural Resources Canada for his vast knowledge of theory, methods and functions of spectroscopy and Dr. Greg Finn for the many years of great instruction, patience and support. I would also like to thank the Earth Science Department at Brock University their assistance, patience and knowledge made this project possible. Thank you all for the assistance you provided at all levels of the research project.

I would also like to thank my entire family for the support they provided me through my entire life and in particular, I must acknowledge my best friend and soon to be wife, Keira, and my Mother. Without their collective love and encouragement, I would not have finished this thesis.

I recognize that this research would not have been possible without the support by Diamonds North Resources Ltd. by their contribution of a vast number of minerals for study and by Mineral Services by their hard work in the analysis of these minerals and express my gratitude to these organizations.

Chapter 1: Introduction

1.1 General Introduction

Reflectance spectroscopy has been used in a wide range of geological exploration techniques such as mapping acidic mine waste (Swayze et al. 2000), regional mineral identification (Clark et al. 2003), and mapping alteration zones (van Ruitenbeek et al. 2006). Kimberlite indicator minerals typically have variations in chemistry that will indicate the likely presence or absence of diamond within kimberlite occurrences. Once mineral grains are collected from kimberlite or picked from drift prospecting samples, they are mounted and analyzed by electron microprobe (Dawson and Stephens 1976, Gurney 1984) to determine the major and minor element proportions. Specific geochemistry in minerals such as pyrope garnet in kimberlite can indicate diamond potential to the exploration geologist.

Reflectance spectroscopy is a non-destructive measurement that can help characterize specific minerals as many have a diagnostic spectrum according to its internal crystal chemistry (Burns 1993; Cloutis 2002; Rost et al. 1975). The presence of the first series transition metal elements (Cr, Fe, Ti, Mn, etc) that will substitute for non-transition metal elements in minerals can also be determined by observing absorption features that exist in the visible light spectrum (Burns 1993).

This study collected a data set of mineral spectra including various types of garnet, olivine, diopside, chromite, ilmenite and ruby. The spectra of these samples were then compared to their respective geochemistry determined by electron microprobe. The purpose of this study was to determine if the depths of specific absorption features, such

as those in pyrope garnet, could be related to variations in transition metal geochemistry, in particular, to the mol % of chromium. During the development of this methodology, it was found that the mineral grain volume needed to be taken into account and thus was also measured. For the configuration of the measurement apparatus, the grain volume is a correction factor that also takes into account the field of view proportion occupied by the grain. It works and is effective because the grains are relatively equant and not flat like micas for instance.

1.2 Thesis Presentation

This thesis is presented as a series of Chapters, one of which is intended as a standalone publication and the others describe mineral identifications that are possible from reflectance spectra characteristics and provide suggestions for further studies.

Chapter 2 provides a general background on the geology of kimberlites and the mantle derived lithologies that are sampled by them. These various mantle rock types incorporated into the kimberlite, such as peridotite, are mantle xenoliths and are brought to the Earth's surface by kimberlite intrusions. The depth, occurrence and mineralogy of these xenoliths are identified along with peridotitic subtypes and how they relate to diamond. A brief explanation of crystal field theory is provided along with the effects that electrostatic fields have on first series transition metals in the molecular lattice of particular minerals. When light is applied to these configurations, some atomic orbitals will become forced away from their natural orientation. The arrangement of atomic orbitals after energy is applied will cause energy differences that can be observed in a mineral's reflectance spectrum.

Chapter 3 is a detailed explanation of the specifications and equipment used in this study including the spectrometer, fiber optic cables and Ocean Optics® operating software. Several of the components used in the main assembly were tested to determine the best configuration for this application. It was necessary to test a few fiber optic cables with different transmission ranges to determine the best range for measurements. Various light sources were tested to resolve which exhibited the least spectral drift and electronic interference during measurements. A number of reference panels made of different materials were tested to determine if it is necessary to use a specialized material for reference measurements or if an inexpensive man-made material such as Teflon or ceramic could be used. The methodology used to obtain spectra, measurements and characterization of grains is offered in this Chapter as well as the post-processing procedure used to measure absorption band locations and depths. A rationalization of the absorption band selection has been provided here to explain why the absorption band was chosen for discussion in the next Chapter. The experimental procedure outlined in this Chapter has been determined to be rapid and reliable. It can be inserted as part of the screening practices for indicator minerals prior to microprobe analysis without introducing much of a delay in the determination process.

Chapter 4 is intended as a standalone publication entitled "Absorption Features caused by Elemental Substitutions in the Reflectance Spectra of Pyrope Garnet, a Kimberlite Indicator Mineral." It discusses the substitution of the transition metal chromium into mantle derived pyrope garnet that form with diamond and found in kimberlites. This Chapter describes one of the minor absorption bands caused by chromium at 689 nm and the depth of this band can be used to predict the mol % of

substituted chromium by using the slope of various grain volume fractions. Results of this work suggest that this method could be used as a field exploration tool to determine the mol % chromium in mantle derived pyrope or as a preliminary measurement tool in the lab before sending samples to be analyzed by electron microprobe.

Due to the limited number of mineral grains available for this study, Chapter 5 titled "Spectral characterization of some naturally occurring kimberlite indicator minerals using visible reflectance spectroscopy" is intended to determine if minerals which share the same molecular characteristics, or are formed in the same genetic environment as pyrope garnet, can be analyzed using the same approach. This Chapter is also intended as a pilot study to determine if the techniques used in this thesis are suitable for other minerals. The same techniques are used in this Chapter for the spectral identification of some minerals such as almandine, grossular, spessartine, forsterite, diopside, chromite, ilmenite and ruby. Some possible explanations for absorption features are provided in each section of this Chapter and are related to the geochemistry of each mineral.

Chapter 6 discusses the general conclusions of this study and the possible applications of the work presented in Chapter 4. It also provides suggestions for further studies involving the minerals discussed in Chapter 5. Various other ore deposits in general have indicator minerals that have not been examined in this study, but could also be examined to determine if a relationship of spectral properties to mineral chemistry can be diagnostic as the one proposed in Chapter 4.

References

Burns, R. (1993) Mineralogical applications of crystal field theory: Crystal field spectra of transition metal ions in minerals. Cambridge topics in Mineral Physics and Chemistry. Cambridge University Press, New York. Pg 1-190

Clark, R., Hoefen, T., Swayze, G., Livo, E., Meeker, G., Sutley, S.,Wilson, S., Brownfield, I., Vance, S. (2003). Reflectance Spectroscopy as a rapid assessment tool for the detection of amphiboles from the Libby, Montana Region *U.S. Geological Survey Open-File Report 03-128.*

Cloutis, E. (2002) Pyroxene reflectance spectra: Minor absorption bands and effects of elemental substitutions. J. Geophysical Research, 107: E6. Pg 1-12

Dawson, J.B., Stephens, W.E. (1976) Statistical Classifications of garnets from kimberlite and associated xenoliths. Addendum. J. Geol., Vol. 84, pg 495-496.

Gurney, J.J., (1984). A correlation between Garnets and Diamonds in Kimberlite. In: Glover, J.E., Harris, P.G. (Eds.), Kimberlite occurrence and origins: A Basis for Conceptual Models in Exploration. Geology Department and University Extension, University of Western Australia, Publication 8 143 – 166.

Rost, F., Beermann, E., Amthauer, G. (1975) Chemical Investigation of pyrope garnet in the stockdale Kimberlite intrusion, Riley County, Kansas. American Mineralogist. Vol. 60 pg 675 – 680.

Swayze, G.A., Smith, K.S., Clark, R.N., Sutley, S.J., Pearson, R.M., Vance, J.S., Hageman, P.L., Briggs, P.H., Meier, A.L., Singleton, M.J., and Roth, S., (2000) Using imaging spectroscopy to map acidic mine waste, Environmental Science and Technology, **34**, p. 47-54.

Van Ruitenbeek, F. J.A. Debba, P. Van der Meer, F.D. Cudahy, T. Van der Meijde, M.Hale, M. (2006) Mapping white micas and their absorption wavelengths using hyperspectral band ratios, Remote Sensing of Environment **102**, p. 211-222.

Chapter 2: Background Geology

2.1 Kimberlite

Diamonds and their indicator minerals are transported from the mantle through the crust and to the surface of the earth by intrusive processes which form a rock type known as kimberlite. Kimberlite is a type of volatile-rich, ultramafic, ultrapotassic volcanic rock type with a complex assemblage of minerals and xenoliths (Skinner and Clement 1979). Grain sizes of these minerals range from < 1mm to 20 cm whereas xenoliths can occur in all sizes (Carlson et al. 2005). Kimberlite consists of a fine-grained matrix rich in various xenoliths and altered by CO_2 and H_2O; the major volatiles within the kimberlitic magma (Carlson et al., 2005). Generally, kimberlites contain approximately 20% magma and 80% accidental material and are suggested to originate deep within the mantle at depths from 300 – 600 km (Field et al. 2008). At this depth the ascending magma samples the deepest parts of the lithosphere. It tends to erupt rapidly and violently with substantial CO_2 and volatile components (Field et al. 2008).

2.1.1 Kimberlite Mineralogy

Kimberlite has a complex and vast mineralogy consisting of a primary assemblage of anhedral olivine, pyrope, enstatite, diopside, ilmenite, phlogopite, chromite and diamond. Olivine is the dominant mineral of this mineral assemblage (Skinner and Clement 1979). Kimberlite is the primary source of diamond on Earth but is still a rare component (Skinner and Clement 1979). These minerals originate from samples of the mantle lithosphere that have become disaggregated upon transport within the kimberlite magma. A secondary generation of minerals is formed during the

generation and ascent of the kimberlite which makes up the matrix and consists of euhedral olivine, phlogopite, monticellite, perovskite and spinel (Skinner and Clement 1979, Carlson et al. 2005).

Kimberlite is restricted to Archean cratons due to the fact that they are often the thickest parts of the earth's crust with low heat flow values (Carlson et al. 2005). As kimberlite magma ascends through the lithosphere, the magma brecciates the surrounding wall rock, including with it various lithologies from the mantle and above (Carlson et al. 2005). They often occur in clusters from 2 to 20 pipes reaching up to 50 km in diameter. Ages for kimberlites worldwide range from 2 Ga to 18 Ma and have increased in intensity but decreased in diamond content throughout geologic time (e.g. Canada, Africa) (Kogarko 2008).

2.1.2 Accidental Xenoliths

Xenoliths are rock fragments within an intrusive igneous body that are unrelated to the igneous magma itself (Winter 2001). These fragments represent older rock incorporated into the magma while it was still fluid (Winter 2001). Mantle xenoliths reflect the temperature, pressure, composition and the differential stress conditions that they have experienced prior to accidental sampling by their host magma. Common types of mantle xenoliths that have been found to occur within kimberlite include, in order of abundance peridotite, eclogite, various xenocrysts, pyroxenite, and ultra-deep varieties of peridotite and deformed / metasomatized variations of all of the above (Carlson et al. 2005).

2.1.3 Peridotite

By definition, peridotites contain at least 40% olivine with clinopyroxene and orthopyroxene (Figure 2.1). It is an ultramafic coarse grained igneous rock with high proportions of magnesium and relatively low amounts of silica (45 wt. %) (Winter 2001). Bulk compositions of these rock types are also known to be depleted with respect to Fe, Ca and Al. Peridotites being the most common rock type occurring as mantle xenoliths are thought to represent the composition of approximately 90% of the Earth's mantle (Carlson et al. 2005).

Peridotites can be further subdivided into 4 separate types as illustrated in Figure 2.1. 1) Dunites which are composed of over 90% olivine with orthopyroxene (Opx) and clinopyroxene (Cpx) being less than or equal to 5%. 2) Lherzolites which are dominated by olivine and have approximately equal amounts of Cpx and Opx (~30%). These are the most common types of peridotite found as xenoliths (Carlson et al. 2005). 3) Wehrlites also have major olivine components but are enriched in Cpx and depleted with respect to Opx. 4) Harzburgites which still have major olivine proportions but are enriched in Opx and depleted with respect to Cpx. Diamonds have been identified to form generally within harzburgitic peridotites however it has also formed in minor amounts in others (Carlson et al. 2005).

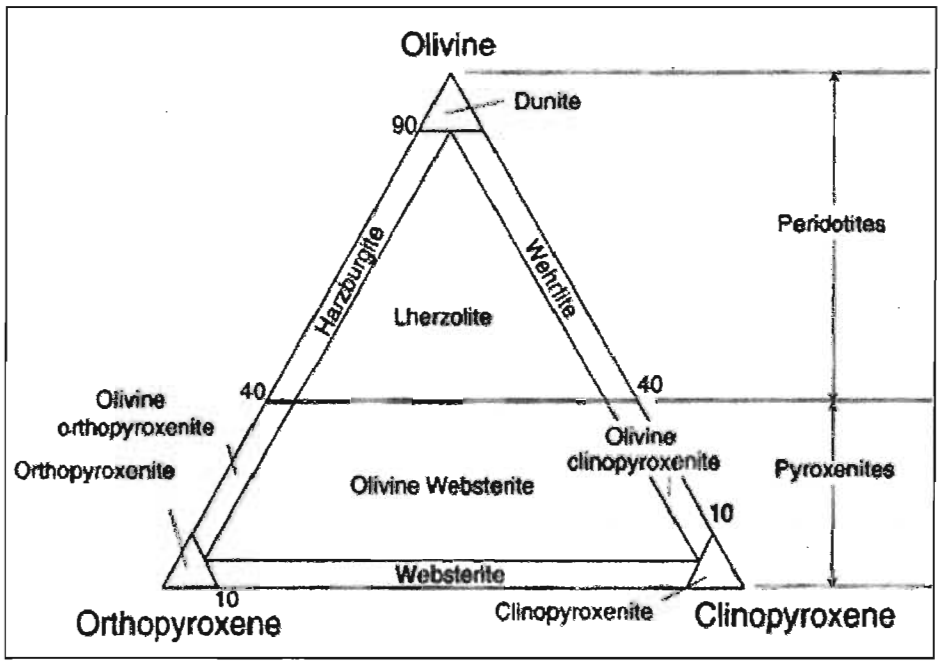

Figure 2.1: Ultramafic classification diagram based on proportions of olivine and pyroxene in the rock allowing us to differentiate between peridotite and pyroxenite. The corner at the top represents 100% olivine, the bottom left corner represents 100% orthopyroxene and the bottom right corner represents 100% clinopyroxene (Winter 2001).

The geological occurrence of the different types of mantle related xenoliths are illustrated in Figure 2.2. Beneath the lithospheric - asthenospheric boundary, the approximate location of a subducted oceanic slab is illustrated which has already undergone metamorphism into an eclogite.

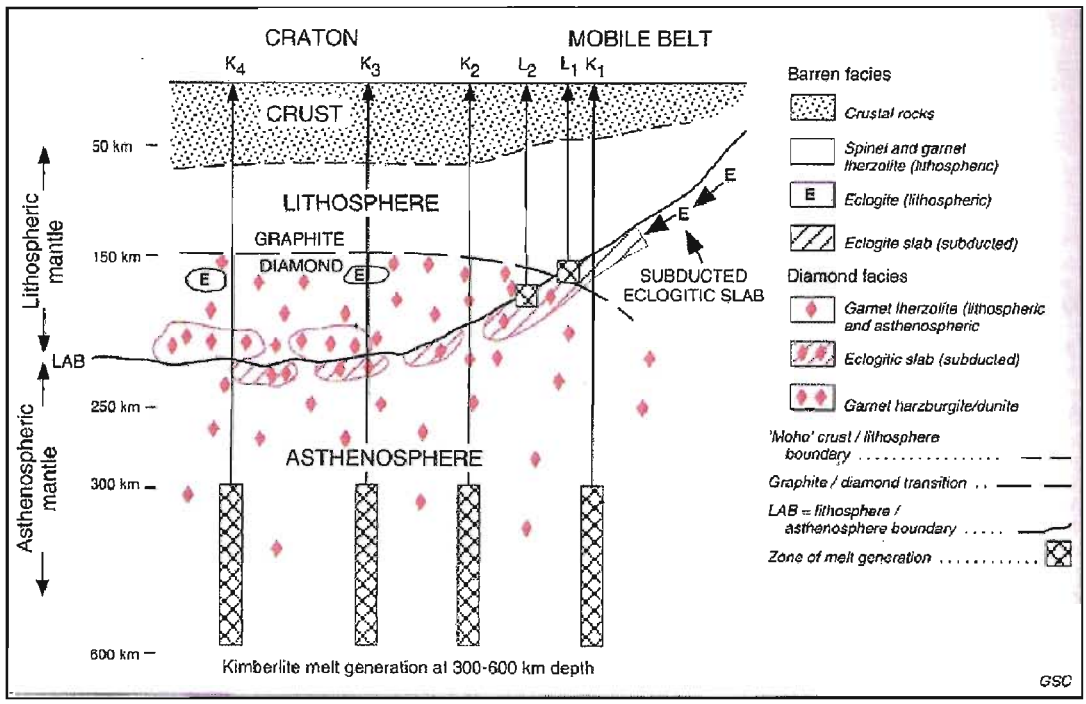

Figure 2.2: A general cross-section of an ancient craton indicating kimberlite paths (K) and subducted oceanic eclogite paths (E) and graphite-diamond phase changes relative to the lithospheric and asthenospheric boundaries. Lamprophyre (L) is another type of volcanism not involved in this study (Modified from Eckstrand et al. 1995).

2.1.4 Xenocrysts

Xenocrysts are minerals in an igneous rock which have not crystallized from the melt but have been introduced into the melt from an external source (Carlson et al. 2005). Common mantle xenocrysts that may form with diamond include olivine, pyrope, enstatite, diopside, ilmenite, chromite and spinel. These minerals are termed indicator minerals, indicating the potential presence of diamond. Although there are many minerals that are xenocrystic in kimberlitic melts, not all may be present in each kimberlite. The proportions of these minerals vary and differ from pipe to pipe as each may sample different lithologies or mantle sections (Kogarko 2008, Field et al. 2008).

Important aluminum bearing mineral phases present in ancient cratons are spinel from 50 – 80 km and garnet from over 80 km depths (Carlson et al. 2005, Eckstrand et al. 1995). Below the lithospheric boundary are representations of kimberlitic melts and the paths that they take sampling material above. The dominant rock type found in the mantle lithosphere is lherzolitic peridotite. Harzburgitic peridotite varieties are found in lesser amounts and are well known to contain diamond which forms at depths greater than 150 km (Carlson et al. 2005, Eckstrand et al. 1995).

2.2 Diamonds

Diamonds are rare polymorphs of carbon that crystallize in the mantle at temperatures of ~900 – 1000°C and pressures over 50 kilobars or 150 km depth (Carlson et al. 2005). The crystal lattice is known to be almost entirely covalently bonded carbon atoms with minor impurities (Carlson et al. 2005). This strong type of bonding helps denote diamond as the hardest natural substance. As the presence of impurities increases the diamond lattice decreases in bond strength (Carlson et al. 2005). Diamonds are discrete mantle xenocrysts, typically forming in peridotite and eclogite within the Archean subcontinental lithosphere. These mantle samples are transported from great depths by explosive kimberlite activity throughout geologic time (Carlson et al. 2005).

2.2.1 Geological Setting of Diamonds

The formation or transition of diamonds from graphite requires high pressures at moderate temperatures, and even higher pressures at high temperatures (Carlson et al. 2005). This is why they are restricted to old continental cratons as in Figure 2.2. The low geothermal gradient under old cratons decreases the pressure of this transition, and

allows diamonds to be preserved and carried to the surface by kimberlite pulses (Carlson et al. 2005, Klein 2008).

2.2.2 P-type Diamonds

P-type diamonds can be defined as diamonds which form from a mantle related melt in association with mantle related peridotite and are found primarily within harzburgitic peridotites. Mineral inclusions are visible within most diamonds. These inclusions form syngenetically with diamond and indicate what type of mantle environment existed during formation. Peridotites comprise approximately 95 % of the Earth's mantle, so it is thought that most diamonds occur in this rock type (Carlson et al. 2005). Mineral inclusions identified in P-type diamonds are Cr-rich pyrope, Cr-rich diopside, enstatite, chromite and olivine. When these minerals are found interstitially within kimberlite they are classified as indicator minerals, indicating the possible presence of diamond (Klein 2008, Carlson et al. 2005).

P- type diamonds can be further subdivided into harzburgitic or lherzolitic based on the extent of depletion indicated by the Cr_2O_3 and CaO content of their included garnet (Figure 2.3) (Carlson et al. 2005). Illustrated in Figure 2.3(a) are ~900 garnet samples from a variety of identified xenoliths obtained from kimberlite. The line through the diagram indicates a positive correlation of Cr_2O_3 and CaO. Garnets below this line are harzgurgitic and above it are lherzolitic and wehrlitic. Samples that run along the CaO axis are eclogitic. Figure 2.3(b) shows these fields much clearer indicating that harzburgites have much higher Cr_2O_3 contents and lower CaO, lherzolites and wehrlites have a 1:1 correlation and eclogites having higher CaO and very low Cr_2O_3 contents.

Research involving the inclusions in diamond has suggested that diamonds form syngenetically with harzburgitic peridotites (Carlson et al. 2005).

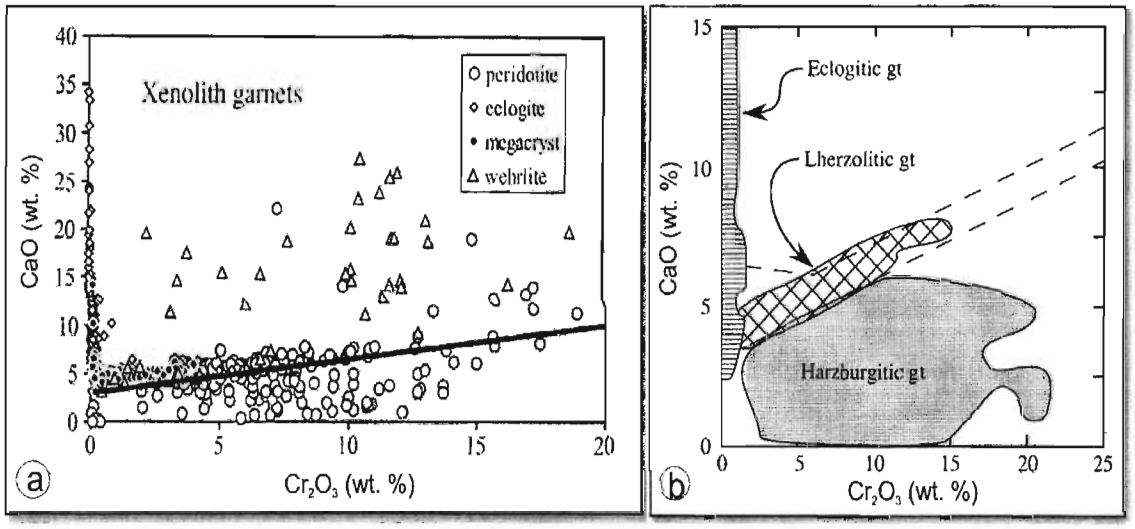

Figure 2.3: Graphs for CaO vs Cr_2O_3 values measured in pyrope garnet obtained from kimberlite and inclusions in diamond. (a) - Approximately 900 samples of garnet. Garnets formed in association with harzburgites lie below the line and above the line are lherzolites. (b) - Enlargement of (a). These plots aid in the determination of diamond bearing xenoliths such as harzburgitic varieties (Carlson et al. 2005).

2.2.3 E-Type Diamonds

E-type diamonds are classified as such when the diamond mineral inclusions match the mineralogy of an eclogite. E-type diamonds form in subducted oceanic crust that has undergone metamorphism of depths below the graphite-diamond transitional boundary (~150km) (Figure 2.2) (Eckstrand et al. 1995). The evidence as to the origin of these diamonds is found within mineral inclusions such as pyrope – almandine – grossular garnet, omphacite and kyanite. Trace elements that are preserved in the mineral such as nitrogen and boron and the carbon isotopic composition can be a further indication of the parent rock type the diamond formed with. The higher nitrogen content in E-type diamonds suggests a faster growth rate compared to P-type diamonds and could

also be an indication of primordial nitrogen contents of the primitive mantle but is beyond the scope of this report (Carlson et al, 2005). Numerous studies on the carbon isotopic composition of E-type diamonds have attempted to provide an understanding as to their origin. P-type diamonds have been determined to have a constricted range in carbon isotopic compositions that include relatively heavy carbon isotopes. In contrast, E-type diamonds have been illustrated to have a much broader range in carbon isotopic composition, including mainly those with light carbon isotope values and rarely heavy isotopes (Carlson et al. 2005). These light carbon isotopes in E-type diamonds are characteristic of organic matter that must have been subducted along with an oceanic plate. Heavy isotopes of carbon that have been identified in these diamonds have been attributed to marine carbonate (Carlson et al. 2005).

2.3 Crystal Field Theory

Crystal field theory is defined as a way to describe the result of changes in the d-orbital energy levels of a transition metal ion (Burns 1993). These changes are caused by electrostatic fields that originate from negatively charged anions known as ligands that are positioned on a lattice about a transition metal ion.

The effect on a particular transition metal ion depends on the type, position and symmetry of these surrounding ligands (Burns 1993). The definition of a transition element is a metal having incompletely filled d-electron orbital shells. More accurately they are those elements that have partially filled d-orbitals in one of their commonly occurring oxidation states (Burns 1993). The elements include those in the first series of the periodic table: scanadium, titanium, vanadium, chromium, manganese, iron, cobalt,

nickel, and copper. Their electronic configuration is $(1s)^2(2s)^2(2p)^6(3s)^2(3p)^6(3d)^{10-n}(4s)^{1\text{ or }2}$ or simply [Ar] $(3d)^{10-n}(4s)^{1\text{ or }2}$ where n = numbers 1 to 10 (Burns 1993). Moving from one element to the next along the first transition series the 3d orbitals are progressively filled. The different oxidation states of various cations are formed due to the presence or absence of some 4s or some 3d electrons (Burns 1993).

2.3.1 d orbitals

The five d orbitals that are present in each shell are designated by the terms d_{xy}, d_{yz}, d_{xz}, $d_x^2\text{-}_y^2$, and d_z^2. These orbitals have four lobes in opposite quadrants. Orbitals may be split into two main groups due to the angular distributions of their lobes (Burns 1993). Three of these orbitals, d_{xy}, d_{yz}, d_{xz}, are projected in between three Cartesian axes and the other two orbitals, $d_x^2\text{-}_y^2$, and d_z^2 have lobes that project directly on these Cartesian axes. Each one of these orbitals is capable of accommodating two electrons which must be spinning in opposite directions (Burns 1993). This gives the five d orbitals up to a maximum of 10 electrons. When there are not enough electrons in an atom to completely fill a set of orbitals, the electrons may spread out and occupy as many orbitals as possible aligning their spins to parallel. This arrangement minimizes repulsion and leads to the lowest energy states which have the maximum number of unpaired electrons (Burns 1993, Chang 2007).

When six ligands are positioned about a transition metal ion in octahedral coordination, the electrons are repelled in all five 3d orbitals by the negatively charged anions (Burns 1993, Chang 2007). Electrons in the $d_x^2\text{-}_y^2$, and d_z^2 orbital group run along axes towards the ligands and are repelled to a greater extent than those in the group of

three (d_{xy}, d_{yz}, d_{xz}) that point between the ligands (Chang 2007). Therefore these two orbitals are raised in energy relative to the others.

The difference in energy between the two groups is termed the crystal field splitting and is designated by Δ_o. This value may be determined through direct calculations or can be estimated from spectral measurements of transition metal-bearing phases in the visible to near-infrared region of the electromagnetic spectrum as absorption bands (Burns 1993). Examples of these absorption bands are detectable in various types of garnet that are host to a few first series transition metal elements. These elements can exist as major elements as those in almandine (Fe^{2+}), spessartine (Mn^{2+}) and uvarovite (Cr^{3+}) or as minor substituting elements which could be any combination or proportion of those mentioned above (Burns 1993). Studies involving almandine garnet spectra have suggested a few absorption bands in the visible spectral region (VIS) at ~505 nm, ~575 nm and 695 nm are due to the quantity of Fe^{2+} that is included within the almandine crystal structure (Burns et al. 1993; Manning 1967). Absorption bands located in the VIS at ~410 nm, ~565 nm and ~690 nm have been attributed to the chromium that substitutes for aluminum in the pyrope crystal structure (Rost et al. 1975). An absorption band in the VIS located at ~405 nm is attributed to the Mn^{2+} in the spessartine crystal structure (Manning 1967). Most of these diagnostic absorption features are in the ultraviolet, visible and near infrared wavelength range, hence our instrument in the VIS-NIR (mostly VIS) is ideally suited to study these contributing absorption features in garnet minerals.

References

Burns, R. (1993) Mineralogical applications of crystal field theory: Crystal field spectra of transition metal ions in minerals. Cambridge topics in Mineral Physics and Chemistry. Cambridge University Press, New York. Pg 1-190.

Carlson, R.; Holland, H.; Turekian, K. (2005) The Mantle and Core: Mantle Samples include in volcanic rocks: Xenoliths and Diamonds. Elsevier Ltd. Pg 271.

Chang, R. (2007) Chemistry: Ninth Edition. McGraw-Hill Companies Inc. Pg. 288-290 & 949-950.

Eckstrand, O.R., Sinclair, W.D., and Thorpe, R.I., eds., 1995, Geology of Canadian Mineral Deposit Types. Geology of Canada, No. 8. Geol. Surv. Can. Pg 559-567.

Field, M.; Stiefenhofer, J.; Robey, J; Kurszlaukis, S. (2008) Kimberlite-hosted diamond deposits of Southern Africa: A review. Elsevier. Ore Geology Reviews. Vol. 34 pg 33-75.

Klein, C.(2002) The 22rd Manual of Mineral Science. John Wiley and Sons Inc. U.S.A. Pg 347-350.

Kogarko, L.N. (2008) Kimberlite Magmatism in the Earth's History: Diamond Potential and Genesis Pleiades Publishing, Ltd., Doklady Earth Sciences, 2008, Vol. 418, No. 1, Pg. 73–75.

Manning. P.G. (1967) The optical absorption spectra of the garnets almandine, pyrope and spessartine and some structural interpretations of mineralogical significance. Canadian Mineralogist. Vol 9. Pg 237- 251

Rost, F., Beermann, E., Amthauer, G. (1975) Chemical Investigation of pyrope garnet in the stockdale Kimberlite intrusion, Riley County, Kansas. American Mineralogist. Vol. 60. Pg 675 – 680.

Skinner, E.M.W; Clement, C.R. (1979) Mineralogical Classification of Southern African Kimberlites. Second International Kimberlite Conference, Santa Fe, American Geophysical Union. Pg 129-139.

Winter, J.D. (2001) An Introduction to Igneous and Metamorphic Petrology: 19.3.3 Kimberlites. Pearson Education/prentice Hall. Pg 427.

Chapter 3: Experimental Procedure

3.1 Instrumentation

Analyses of individual mineral grains was carried out using an Ocean Optics USB4000-visible to near-infrared (VIS-NIR) Miniature Fiber Optic Spectrometer that is preconfigured with a DET4-350-1000 detector and order-sorting filter to cover the wavelength range from 200-1100nm. This spectrometer features a standard SMA-905 connector, a multi-bandpass order-sorting filter and a 25μm entrance slit for an optical resolution with a field width at half maximum of approximately 1.5nm. The spectrometer collects 3648 samples over the effective wavelength range at 0.335 to 0.365nm intervals. A VIS-NIR fiber optic cable with two SMA-905 connectors and a fiber core diameter of 600 μm and 25 cm in length was employed. Given that the attenuation of the signal increases with increasing cable length, apparatus was configured to minimize the length of cable required for maximum performance. The optimal transmission range of this cable is greatest between 400-950nm (Figure 3.1). The Ocean Optics spectrometer is connected via USB cable to a standard computer and controlled by SpectraSuite™ , a modular Java-based software platform provided by Ocean Optics designed for use with this spectrometer.

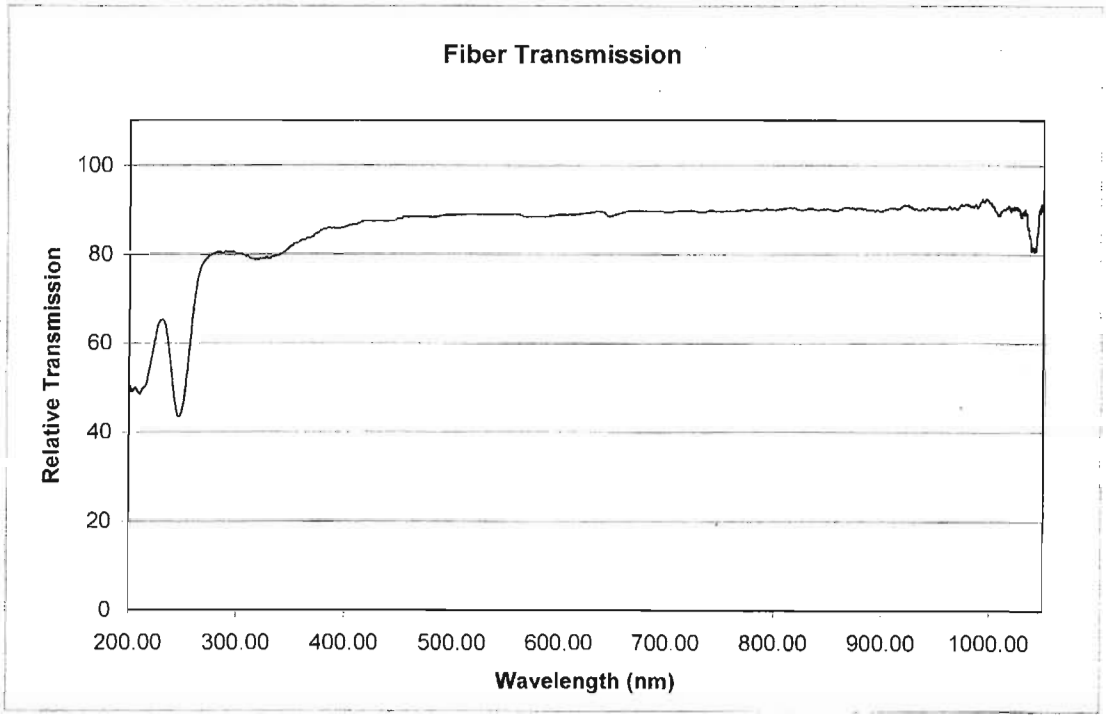

Figure 3.1: Plot of Fiber Optic cable transmission (Provided by Ocean Optics).

For illumination of the mineral grains, resistance-based light sources that change the colour of illuminated light rather than the intensity of the light proved to be unstable and showed greater drift due to electronic circuitry. As a result, a fiber optic 150W quartz halogen light source fixed with a mechanical iris was used in this study. Light is carried from this source to the stage through a dual branch semi-rigid light guide (a fiber optic capable of operating in the VIS-NIR) with a 0.281 inch diameter fiber bundle (Dolan-Jenner fiber-lite EEG2818) and a length of 50 cm. The length of these cables were kept as short as possible given that the shorter the fiber optic cable the less attenuation for both transmission and receiving of light. A plot of the light source gain is given in Figure 3.2 to illustrate the range in wavelength for the light bulb used in this study.

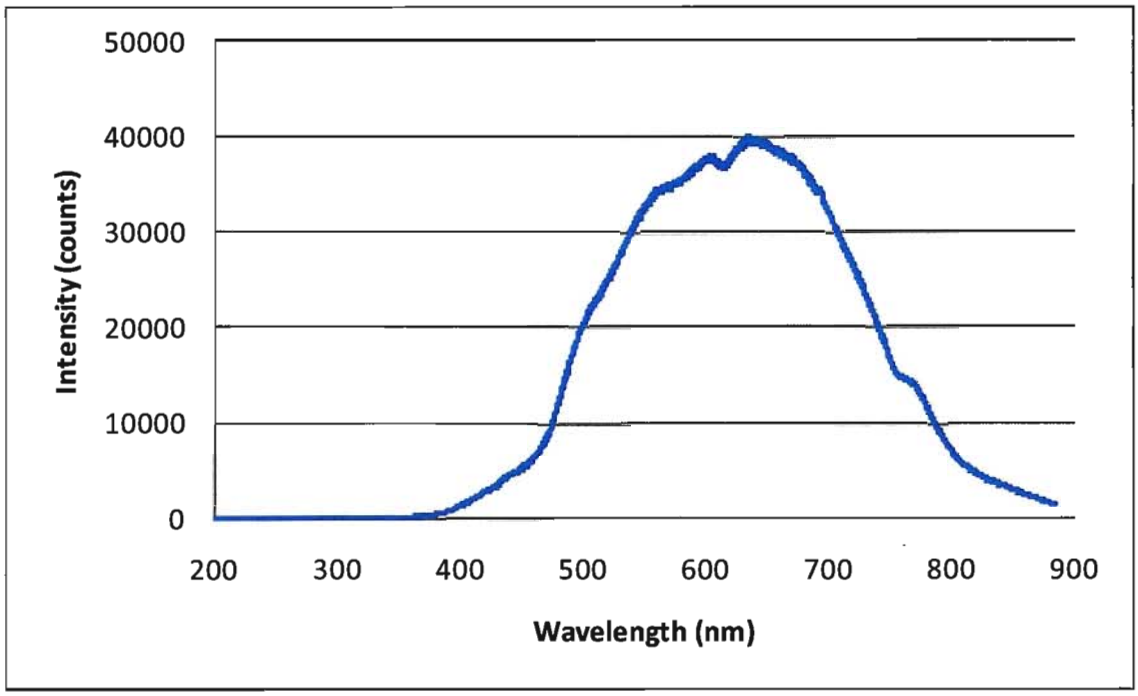

Figure 3.2: Plot of light source gain

A Sony DFW-SX900 Digital Interface Camera equipped via C-Mount with an Edmund optic VZM™ 200i lens are mounted to a 3-axis adjustment stand and can observe the sample on the stage with live feed as the spectra is measured. The working focal distance of the lens with the camera is 9 cm which enabled the camera to take detailed pictures of each grain but not to interfere with the measurement target. Other features include a manual locking iris, the range in the field of view (3.0mm to 12.0mm) and the range in magnification (0.5X to 2.0X). The camera is set at an angle of 10° to the plane of the sample holder (reference plate) with a minimum field of view of 3 mm.

An old microscope body was modified to house the fiber optic cable in the ocular tube. The light sources dual branches are mounted to the stage so that they are in a fixed position pointed directly from both sides towards the grain being measured. The

spectrometer is mounted on top of a modified aluminum microscope assembly (Figure 3.3). The distance from the fiber optic cable to the sample stage can be adjusted to allow various grain size measurements.

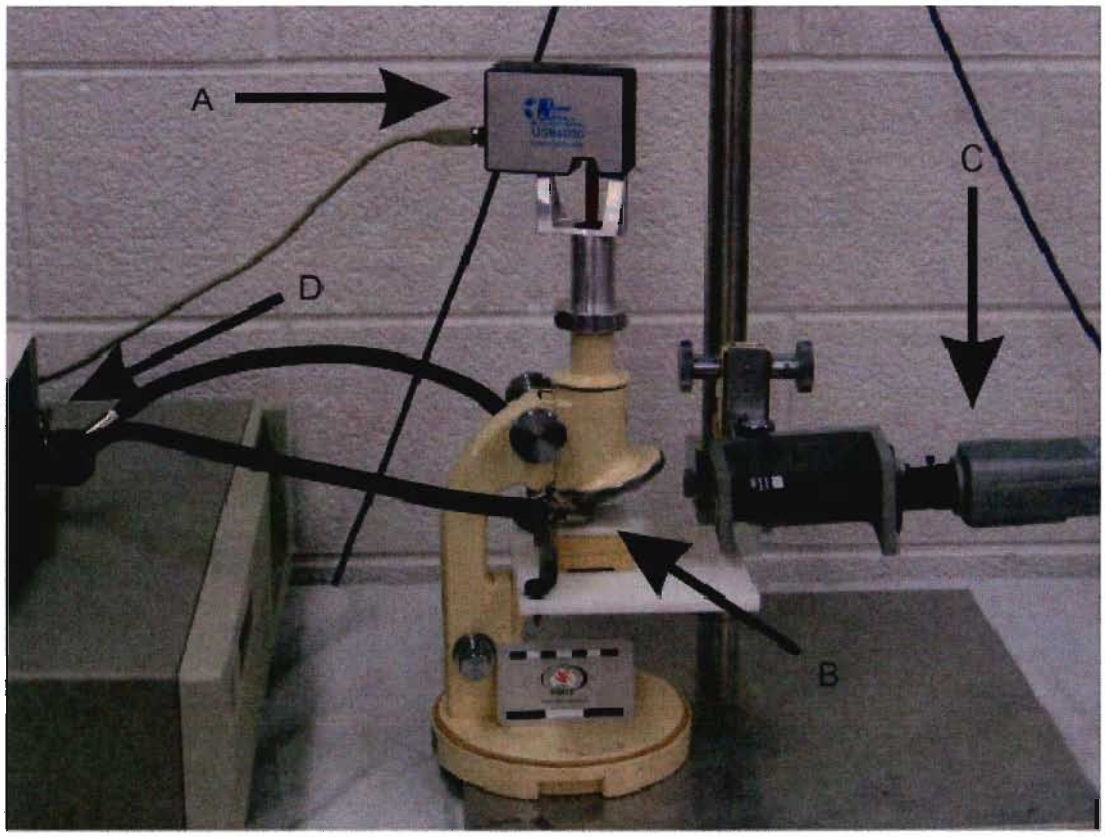

Figure 3.3: Laboratory setup of Spectrometer and materials. A: USB4000 spectrometer. B: Sample stage and optic cable. C: Digital camera. D: Light source

3.2 Methodology

3.2.1 Selection of Reference Panel

Three different types of reference material used in this study include a white ceramic streak plate, a Teflon disk and a Spectralon™ reference panel. Since we are working primarily in the visible light region of the electromagnetic spectrum there is no

need for a reference target with a high near infrared reflectance such as Spectralon. This substance popularly used for measuring spectra is fragile and very porous. The disadvantages of using this material are contamination due to the exchange of grains with tools and the high susceptibility to resting grains leaving pocks and marks. It also needs constant polishing with sandpaper or emery paper to keep clean which adds to the overall maintenance and time needed to take measurements. The high expense of this material would not be beneficial to this type of study since the analyst would have to keep maintaining or replacing the Spectralon panel due to the need of requiring the reference panel to also serve as the sample holder

The use of a Teflon reference panel worked well as a white reference as it is very close to the Spectralon composition. The problem with this material is that Teflon built up static electric charge when exposed to light which made it difficult for grains to remain in the sample well.

A white ceramic plate had good reflectance characteristics in the VIS with respect to the Spectralon but a minor anomalous artifact feature in the range of 690 to 696 was recognized. This artifact was attributed to impurities in the composition of the ceramic. Corrections for this artifact, was made using an Excel macro was necessary due to the proximity of the artifact with respect to the absorption feature of interest. The artifact was very close to the researched absorption feature but did not interfere with it. Confirmation of the proximity of this artifact to the absorption feature was accomplished using the Spectralon. Continuity across the artifact was achieved using a linear interpolation.

3.2.2 Spectral measurement methodology

Prior to placing the grain on the stage for measurement, scans are set at 40 ms and 10 scans are averaged together which reduces the amount of system noise that is visible on the spectral graph. The dark current signal that consists of the thermal instrument and internal electrical noise that contributes to this background signal was removed.

The value of the gain was set at 40,000 counts, well below the saturation maximum of about 65,000 from the reference target material but high enough to obtain a good signal to noise ratio. The Teflon and ceramic plate were both used here for the white reference targets. Samples are measured on this reference material in a 0.1mm well. Measurements are converted to % reflectance based on normalization to the pure white reference spectrum. This normalizes the spectral graph to the reference. Measurement of the reference panel must be repeated every few measurements to check for stability. This is because of the variation in the intensity of the light source and instrument drift.

3.3.3 Grain characterization

Each grain must also be measured and observed to determine grain size, shape and any visible inclusions, rims or alteration. This is for the reason that light can be not only scattered and absorbed by internal imperfections and inclusions but can also be affected by the internal path length that light takes as it propagates through a medium. These factors can affect the magnitude of absorption features and possibly cause anomalous features from other associated minerals. These measurements are made using a digital electronic caliper with a resolution of 0.01mm with an accuracy of 0.03mm. Each grain is centered on the ceramic reference panel and set directly beneath the fiber

optic cable and a reflectance measurement is recorded. Due to fractures and irregularities on the surface of the grain scattering in various directions may occur reducing the amount of light reflected from the sample. The grain is moved under the fiber optic cable until the maximum depth of absorption is observed in real time using the spectral graph.

Five measurements of each individual grain are made at different orientations to obtain a complete dataset. At each orientation an image is taken to further observe grain size, shape, colour and any inclusions visible within the grain. It takes less than 2 minutes to take all measurements and pictures as well as make any observations visible in each image (Figure 3.4).

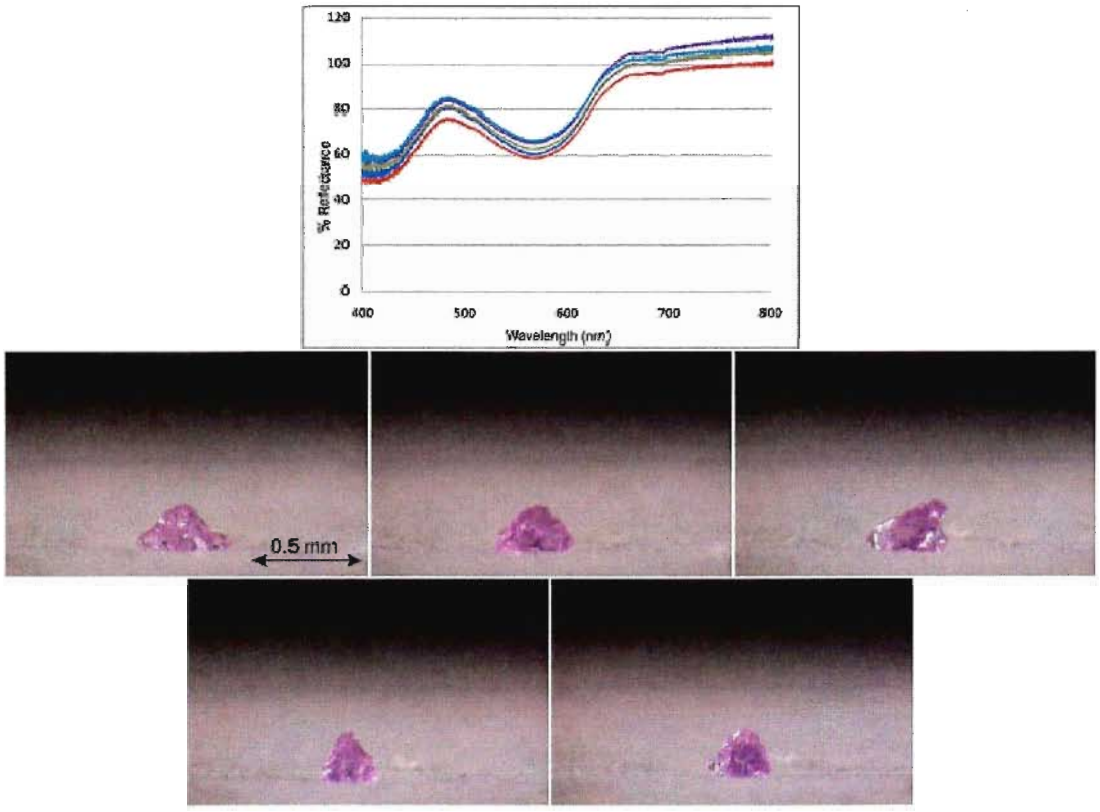

Figure 3.4: Spectral graph of one pyrope garnet at 5 various orientations. The images below the graph show the garnet in each orientation. The fiber optic cable which leads to the spectrometer is positioned directly above the grain.

3.3.4 Post-Processing

After all measurements and observations have been taken, the results are entered into an Excel spreadsheet. Data is normalized with a Gaussian filter and a spectral artifact resulting from the use of the ceramic sample holder is removed with an in-house designed Excel VB macro. Once all data is normalized spectral data is processed in a spreadsheet to measure depth profiles, slopes and wavelength locations of absorption bands after removing the continuum (Clark 1999). The continuum is removed automatically in this VB macro by calculating a straight line tangent to the reflectance spectrum from the maximum value of the left shoulder to the maximum value of the right shoulder. Values are subtracted from this line to produce a value of 100% reflectance on either side of the absorption feature. The depth is calculated as the value in % reflectance from the deepest point of the absorption feature up to the continuum line. For brevity, absorption features in this study are identified by the wavelength of their maximum depth. For example, Ab 689 is the absorption feature centered about 689 nm.

3.3.5 Chemical Analysis

The chemical analyses of the mineral grains used in this study have been determined using the electron microprobe by Mineral Services. The complete dataset is given in elemental weight % and is available in the appendix (see MS10_016). For the purpose of this study each mineral's weight % has been converted to mol % for clarity and a more accurate representation of the effect of elemental proportions on the spectrum of a mineral grain.

3.3.6 Absorption Band Selection

The spectrum of pyrope garnet contains more than one absorption feature for the transition metal chromium in the visible light spectrum as illustrated in Figure 3.5. The two wide features located at 423nm and 577nm are due to crystal field transitions of Cr^{3+} in octahedral coordination in the M1 crystallographic site (Cloutis 2002). The third narrow feature at 689nm could be due to crystal field transitions as mentioned by Cloutis (2002) at the same wavelength for chrome diopside or could possibly be due to spin-forbidden crystal field transitions. Further study on this absorption feature will indicate its cause. These absorption features are not only observed to increase as a result of an increase in Cr^{3+} in this study but also in other studies such as those undertaken by Rost (1975).

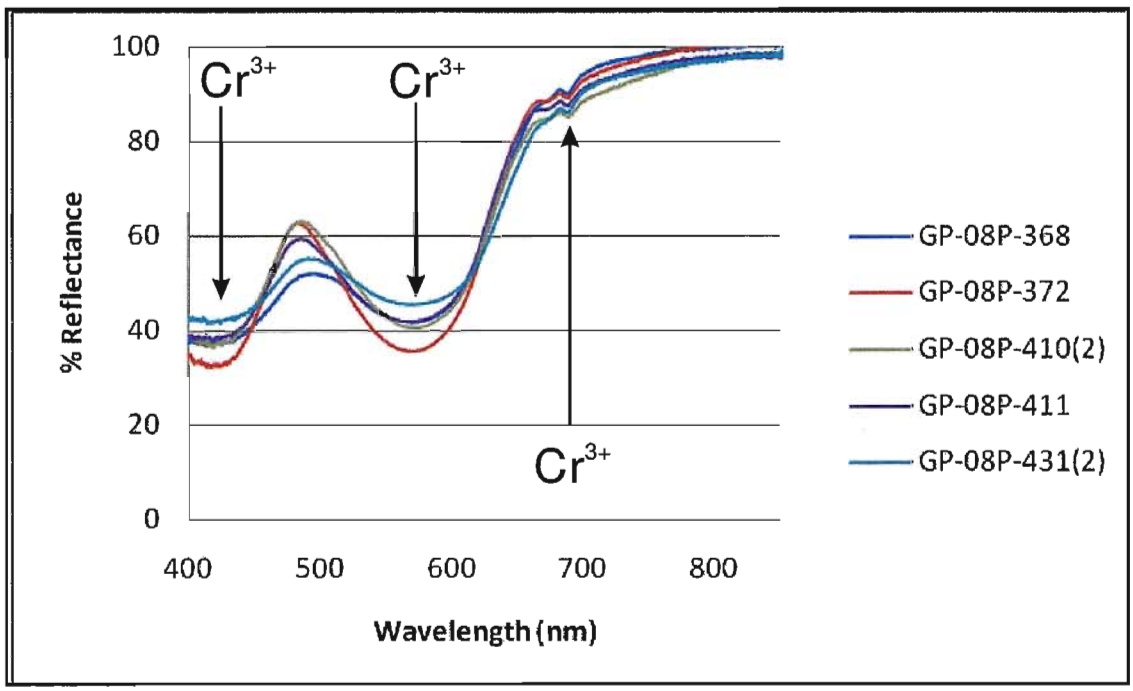

Figure 3.5: The reflected spectrum of 5 chrome pyrope garnets with various Cr_2O_3 proportions. Absorption features have been labeled with transition metals that have been reported from Rost (1975) and observed in this study.

The absorption feature located at 410 nm lies on the margin of the sampling range of the fiber optic cable used in this study. This makes it impossible in this study to determine the exact absorption depth across the continuum. The other absorption features (577nm, 689 nm) can both be measured with respect to their continuum removed depth profiles. Using the 30 pyrope garnets obtained from the same mantle xenolith we can assume a relatively constant proportion of molecular chromium in each sample so that only the grain size and absorption depth will change. The graphs illustrated in Figure 3.6 are evidence that the depths of these absorption bands are not only affected by chromium proportions but are also affected by the size of the grain being measured in volume. Grain volume was calculated by first measuring the three axes of each grain with a digital electronic caliper having a resolution of 0.01mm and accuracy of 0.03mm. This was followed by using the calculation for the volume of an ellipsoid for each mineral grain:

$$V=4/3\pi\, r_1 r_2 r_3$$

where r_1 r_2 $r_3$each represent one of the measured axes.

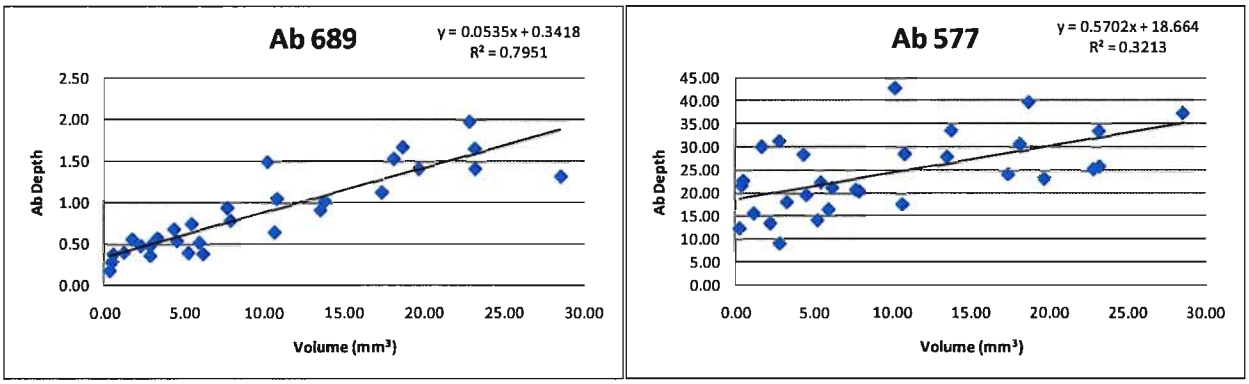

Figure 3.6: Two graphs illustrating a clear linear relationship as defined by the trend line plotted through the data. The trend line for Ab-689 has a correlation coefficient (R2 value) of 0.795 indicating that as grain size increases, the absorption depth will increase linearly. A comparison with Ab 577 has been shown with the same relationship as the above however the R2 values are much lower (0.321) indicating that others factors are contributing to larger absorption bands.

The definite trend from Ab-689 to Ab-577 is the increase of scattering of the data from the narrow to the wide absorption band. This may be due to the magnitude of the large Ab-577. The width of this band can include many smaller absorption bands that are attributed to other transition metal elements. Although the majority of the light absorbed throughout these wavelengths are attributed to Cr_2O_3 the amount of noise and scattering of the data in the plots on the right indicate that the depths for Ab-577 cannot be correlated to changes in grain volume. Although the two absorption bands at 577 and 689 nm can both correlate to the transition metal chromium, only the small band at 689 nm can be associated with differences in volume at a roughly constant Cr_2O_3 molecular percent. The plots provided suggest that the variation in grain size is much clearer using the minor absorption band at 689nm for predicting the amount of chromium in pyrope garnets. This feature is investigated in more detail in the subsequent Chapter.

References

Clark, R. N. (1999), Spectroscopy of rocks and minerals, and principles of spectroscopy, in Manual of Remote Sensing, vol. 3, Remote Sensing for the Earth Science, edited by A. N. Rencz. John Wiley, Hoboken, N. J. Pg. 3 – 58.

Cloutis, E. (2002) Pyroxene reflectance spectra: Minor absorption bands and effects of elemental substitutions. J. Geophysical Research, 107: E6. Pg 1-12

Rost, F., Beermann, E., Amthauer, G. (1975) Chemical Investigation of pyrope garnet in the stockdale Kimberlite intrusion, Riley County, Kansas. American Mineralogist. Vol. 60. Pg 675 – 680.

Chapter 4: Absorption features caused by elemental substitutions in the reflectance spectra of pyrope garnet, a kimberlite indicator mineral

4.1 Introduction

Exploration methods for diamond bearing kimberlites involve the analysis of major and minor element compositions within mantle related indicator minerals. This analysis is traditionally done using an electron microprobe (Dawson and Stephens 1976, Gurney 1984, Grutter et al. 2004) which involves significant sample preparation. Reflectance spectroscopy is a non-destructive analytical method that has many geological applications in a variety of techniques such as mapping acidic mine waste (Swayze et al. 2000), regional mineral identification (Clark et al. 2003), and mapping alteration zones (van Ruitenbeek et al., 2006). In mineralogy, visible light reflectance spectroscopy can help characterize specific minerals (Burns 1993; Cloutis 2002; Rost et al. 1975). One application has been to determine the presence of the first series transition metal elements (Cr, Fe, Ti, Mn, etc) that will substitute for non-transition metal elements in silicate kimberlite indicator minerals (Burns 1993). The purpose of this work is to determine the potential for reflectance spectroscopy to evaluate kimberlite indicator minerals, specifically pyrope garnets. The analytical technique used in this study is accurate, rapid and non-destructive to the mineral measured. The results of this study could potentially be used to confirm or reject garnets that are to be sent for microprobe analysis. Reflectance spectroscopy could be performed as a pre-screening approach in the laboratory or owing to the portability, in an exploration camp in the field for rapid identification of the general garnet mineral chemistry.

A study by Gurney (1984) determined that pyrope crystals that have formed syngenetically with diamond are subcalcic and have relatively high Cr_2O_3 concentrations (~2 – 22 wt. %) compared to those that do not form with diamond. A statistical classification scheme was designed to differentiate between regular pyrope garnet, G9 (high Cr_2O_3, CaO) and pyrope linked to the presence of diamond, G10 (high Cr_2O_3, subcalcic) (Dawson and Stephens 1976, Gurney 1984, Grutter et al.2004). This classification has since been updated by Grutter to include a more precise description of the types of garnet found within kimberlites and how to differentiate between them with reference to microprobe data (Grutter et al. 2004). Although a subcalcic nature of a pyrope is more indicative of a diamondiferous kimberlite, high chromium proportions in pyrope indicate that kimberlites have sampled deep seated mantle peridotite. This study aims to discriminate between pyropes with these higher chromium proportions to send for further analysis.

Although the differentiation between calcic and subcalcic pyrope garnets from spectral reflectance properties is currently uncertain, the Cr_2O_3 proportion in a pyrope appears to behave predictably with respect to its spectral reflectance characteristics in the visible spectral region. Transition metal elements such as chromium included within minerals similar to garnet result in a number of absorption bands in the visible spectral region under reflected light (Burns 1993, Cloutis 2002). These absorption bands are due to the splitting of d-orbital energy levels associated with transition metal elements when located in a crystal field (Clark 1999). These d-orbitals can absorb photons with energies matching the splitting difference which allows electrons to move from a lower level to a higher one (Burns 1993, Clark 1999). These energy levels are determined by the valence

of the element, the symmetry of the crystal field, the metal to ligand distances and the type of ligands in the coordination symmetry (Burns 1993, Clark 1999). These factors vary in every mineral which generates diagnostic absorption bands for specific minerals and in particular specific types of mineral species (ex. pyrope or almandine garnet).

Another factor that can influence the appearance of the spectral reflectance characteristics of the target grain being measured is scattering and absorption of photons by a specific mineral grain due to the size of the grain being measured (Clark 1999). As the size of the mineral increases so does the internal path that the scattering can take according to the Beers-Lambert Law. As grain size increases, greater opportunity for absorption of photons exists within the larger grain and light reflection out of the crystal decreases, yielding a mineral spectrum with better defined bands that indicates its chemistry (Clark 1999, Burns 1993). The shape and magnitude of three chromium absorption bands identified in Figure 4.1 (Rost et al. 1975) depend on a variety of factors including grain size. The two wide features located at 423nm and 577nm are due to crystal field transitions of Cr^{3+} in octahedral coordination in the M1 crystallographic site (Cloutis 2002). The third narrow feature at 689nm could be due to crystal field transitions as mentioned by Cloutis (2002) at the same wavelength for chrome diopside or could possibly be due to spin-forbidden crystal field transitions. Further study on this absorption feature will indicate its cause. These absorption features are not only observed to increase as a result of an increase in Cr^{3+} in this study but also in other studies such as those undertaken by Rost (1975).

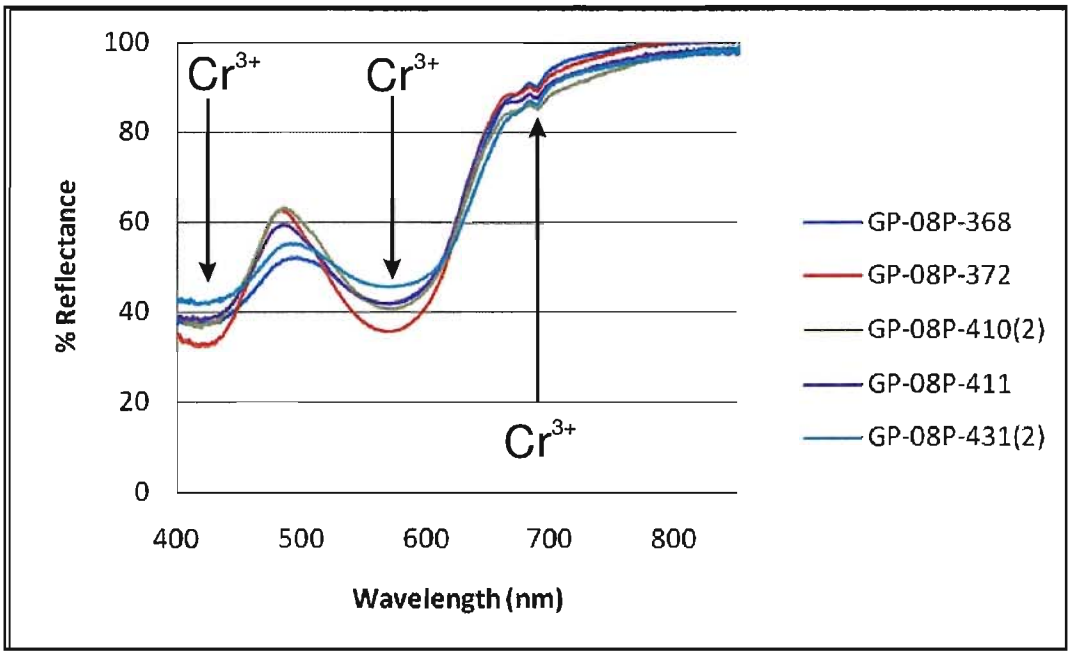

Figure 4.1: A plot of the typical reflectance spectra of 5 chrome pyrope garnets with various Cr_2O_3 proportions as observed in this study and reported by Rost et al. 1975.

This research project focuses on examining the relationship between the depth of certain absorption bands in the visible spectral region that occur with respect to the chromium content from a set of pyrope garnets made available to us. The results of this project may aid in the kimberlite exploration phase by developing a spectral examination technique for garnet indicator minerals.

4.2 Background Science

4.2.1 Garnet Chemistry and Crystallography

The molecular formula for garnet is $X_3Y_2(ZO_4)_3$ where three different coordination symmetries host both transition and non-transition metal elements. This molecular coordination is illustrated in Figure 4.2. The X site is occupied by divalent cations (Mg, Fe^{2+}, Ca) in 8-fold coordination symmetry defined by a distorted cube. The

Y site is occupied by trivalent cations (Al, Fe3+, Cr) in 6-fold coordination defined by a trigonally distorted octahedron (Burns 1993, Deer et al. 1964). Typically the Z site is occupied by Si however trace amounts of Al can occupy this position with 4-fold coordination or regular tetrahedral point symmetry (Deer et al. 1964).

Pyrope is the garnet end-member primarily composed of Mg and Al with variations of other substituting elements. For this reason and the fact that garnet reflects the source chemistry of its origin, it has never been found in the pure state (Deer et al. 1964). Substantial proportions of divalent and trivalent cations will substitute for the major elements and molecules including major proportions of almandine and minor proportions of grossular.

In pyrope and almandine, arrangements of cations and ions resemble distorted cubes. This distortion results in the divalent cation not resting in the center of symmetry of the deformed cube (Figure 4.2). Trivalent cations in slightly distorted octahedral sites are centro-symmetric due to the comparable metal to oxygen distances in all types of garnet (Burns 1993). This similarity can be visualized spectrally for first series transition metals that occupy this site. Absorption bands associated with each transition metal are reflections of the metal to oxygen distances and other crystal field parameters (Burns 1993).

The chromium proportions in pyrope are thought to be the agent causing the purple colour (Carstens 1973). Although this statement is correct, the element is not the only factor that controls the colour. The colour of the mineral is due to a combination of factors that are associated with the transition metal component of the pyrope grain, the

stretching of the bond lengths between metal to oxygen distances due to the size of the elements and the environment in which the mineral has been formed (Carstens 1973). The composition of pyrope garnet found in kimberlite has been determined from many experiments to contain chromium in small amounts (Grutter et al. 2004).

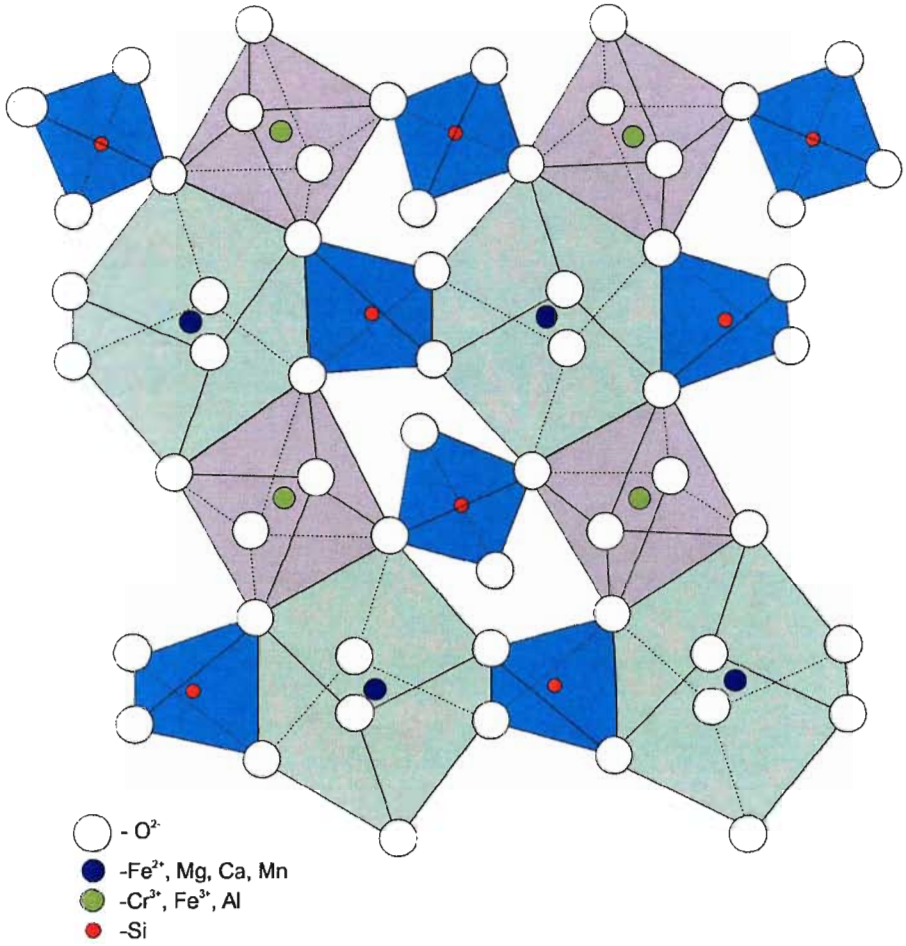

Figure 4.2: A slice of the molecular garnet structure.

4.2.2 Spectroscopy / Crystal Field Theory

Since garnet is a cubic, isotropic mineral, the absorption spectra and crystal field spectra will be equal in all observed orientations (Burns 1993). The variation in garnet spectra observed in the visible to near infrared spectrum is due to transition metals that

substitute in the X and Y crystallographic site. In trace proportions (< 0.25 mol %) these elements will have little influence on the spectra. However, in larger proportions (> 0.25 mol %) these elements will cause absorption bands at specific wavelengths in the absorption spectrum. These wavelengths are based on the crystal field stabilization energy (Burns 1993).

Chrome pyrope spectra in the 400 – 850 nm range are characterized by 2 large absorption bands centered at 410 and 565 nm which have been attributed to crystal field transitions of Cr^{3+} that occupies the M2 (Y) crystallographic site (Rost et al. 1975). It has also been observed to contain a small absorption band at 689 nm (Figure 4.1). The isolation of this narrow band at 689nm, and its uniqueness to chromium is of particular interest to this study. The depths of the larger bands are more pronounced due to the influence of Fe, Mn and other transition metal elements making them difficult to quantify. The smaller absorption band is very narrow, has a high reflection percentage and can be quantified more reliably. Therefore this study will concentrate on the absorption feature located at 689 nm since it may be uniquely related to the presence of chrome substitution.

4.2.3 Grain Size Considerations

Large grains have more internal imperfections and longer internal paths along which light will travel, which increase the amount of photons that are absorbed (Clark 1999). Proportionally, smaller grains have more surfaces for reflection than internal photon paths. Smaller grains have a larger surface-to-volume ratio which is a direct function of grain size. Larger grains will give lower reflectance values and more defined

absorption bands whereas smaller grains will have high reflectance values which may mask these features (Clark 1999).

In our case, for the measurement of individual mineral grains, the increased depth of absorption can be expressed by larger grain sizes. The Beers Lambert Law states that the amount of light being absorbed is proportional to the number of absorbing elements that the light passes through, in thickness (Burns 1993). This law applies for an ideal relationship where the entire field of view is filled by the sample which is not the case in this study. The sample grains used are not large enough to fill the field of view that is being sampled by the fiber optic cable and hence the simple case of the Beers Lambert Law does not apply. For this reason in section 4.4 we examine both the linear size and volume relationship.

4.3 Method and Material

Analyses of individual mineral grains are carried out using an Ocean Optics USB4000 spectrometer and SpectraSuite operating software. The spectrometer is mounted on top of a modified aluminum microscope assembly. Connected to the spectrometer is a 0.25m fiber optic cable which is fixed above the sample stage (Figure 4.3). The distance from the fiber optic cable to the sample stage can be adjusted to allow various grain size measurements. Mounted to opposite sides of the sample stage are two fiber optic cables, both measuring 0.50 m. Short fiber optic cables were chosen to minimize attenuation of the illumination source and transmission of the reflected signal to the spectrometer. The light source houses a halogen bulb and is set at the maximum level. This allows for maximum reflectivity of the sample and consistency from sample

to sample. A Sony digital camera and attached Edmund Industrial Optics objective lens image the grain with a live feed directly on the stage below the fiber optic cable. This is set at an angle of 10° with a minimum field of view of 3 mm.

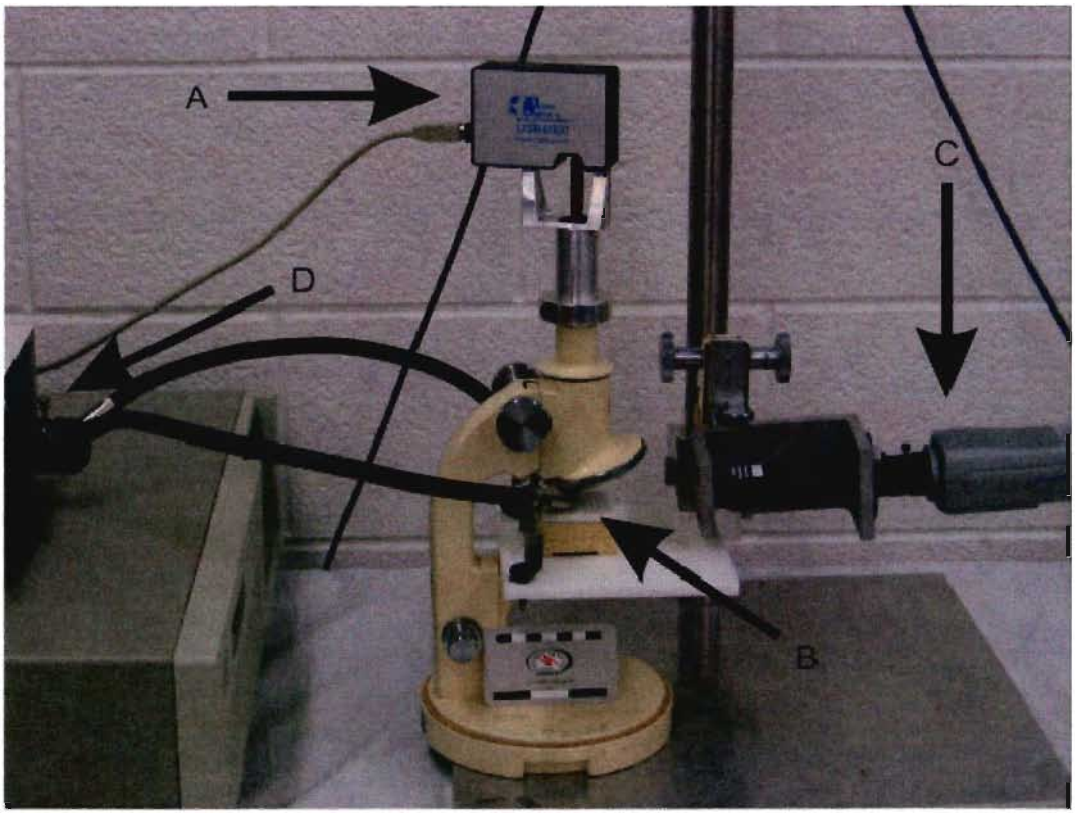

Figure 4.3: Laboratory setup of Spectrometer and materials. A: USB4000 spectrometer. B: Sample stage and optic cable. C: Digital camera. D: Light source

4.3.1 Experimental procedure

Prior to placing the grain on the stage for measurement, scans are set to integrate for 40ms and 10 successive scans are averaged to reduce instrument noise that is otherwise visible on the spectral graph. A white ceramic plate with a small sample well was used as both reference material and subsequent sample holder. Dark and reference spectra are taken at regular intervals in order to monitor changes and correct for thermal noise and instrument drift, as well as for changes in illumination intensity. This ideally

normalizes the ceramic plate to a 100% reflectance reference and must be done every few measurements to maintain consistent measurement quality. Each grain was also measured and observed to determine grain size, shape and any visible inclusions or alterations. The three axes of each grain were measured with a digital electronic caliper with a resolution of 0.01mm and accuracy of 0.03mm. The thickness value for specific tests is measured in the image, perpendicular to the stage directly underneath the fiber optic cable. Each grain is randomly oriented and once the reflectance measurement is made, the grain is physically measured with a digital caliper.

For reflectance measurements, each grain is centered on the ceramic reference panel and set directly beneath the fiber optic cable leading to the detector. Fractures and irregularities on the surface of the grain may scatter light and affect the amount of light reflected from the sample. Relatively stronger absorption by the ceramic plate than the garnet at the longer wavelengths is responsible for reflectance values above 100% when overall reflectance is high. Several comparisons were made and these departures do not adversely affect the calculations of relative absorption depths used in our analysis. Ideally, a Spectralon™ reference panel should be used; however this modified procedure was required due to the soft surface of Spectralon and the large number of measurements required for this study. Improvements and other options were also investigated but are not expanded upon in this report. Grains were slightly moved under the fiber optic cable to ensure that no anomalous reflectance spectra were collected that was not representative. It also assisted in assuring that the maximum depth of absorption features was being collected.

As light is reflected from each grain, the spectral data is observed in real time on screen in the visible spectral region. Five measurements of each individual grain are made at different orientations to obtain a representative spectral sampling for the dataset. At each orientation a digital image is taken to document grain size, shape, colour and any inclusions visible within the grain. It takes less than 2 minutes to take all measurements and photographs as well as to note any observations visible in each image (Figure 4.4). The similarity of reflectance spectrum is typical for all grain orientations, reinforcing the reliability of these measurements. The subsequent spectra used in the analysis discussed below are always an average of all five measurements made from each grain.

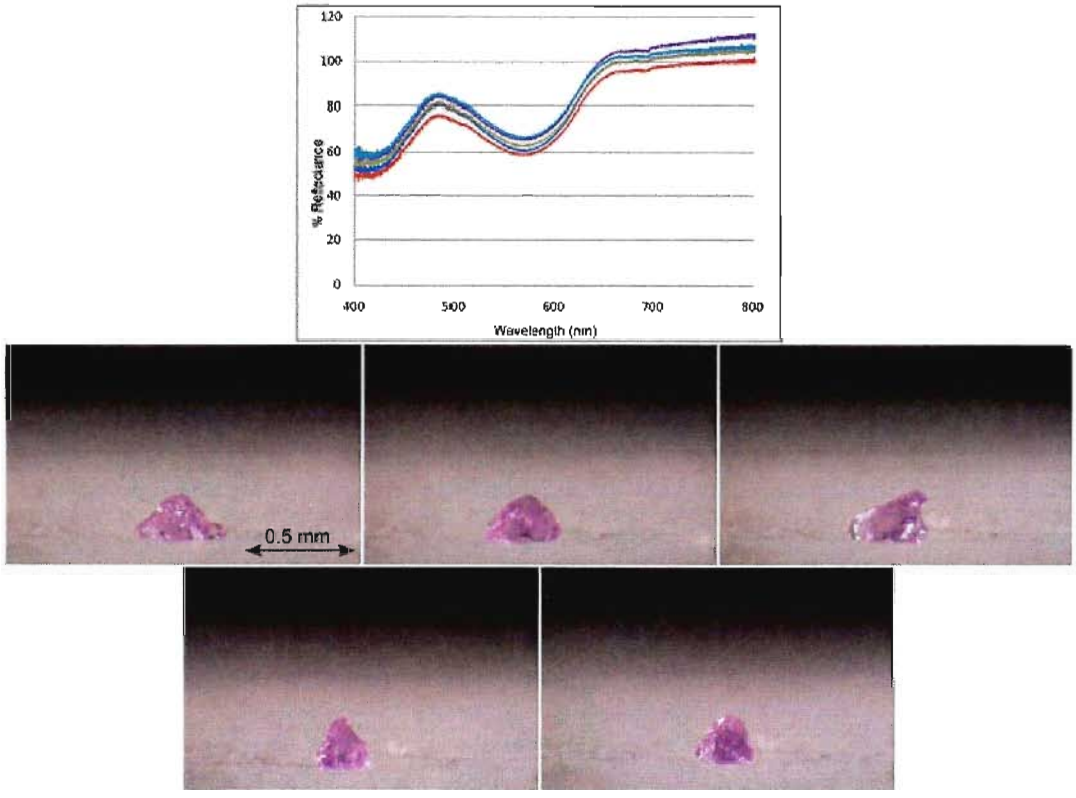

Figure 4.4: Spectral reflectance is graphed for one pyrope garnet in five different orientations. The images below the graph show the garnet in each orientation. The fiber optic cable which leads to the spectrometer views directly above the grain.

4.3.2 Spectral Normalizing and Post-process Filtering

After all measurements and observations have been taken, data for each mineral sample is entered into an Excel spreadsheet. Data is normalized with a Gaussian filter and a spectral artifact resulting from the use of the ceramic sample holder is removed with an in-house designed Excel VB macro. Once all data is normalized spectral data is processed in a spreadsheet to measure depth profiles, slopes and wavelength locations of absorption bands after removing the continuum (Clark 1999). The depths of each absorption band are calculated as a percentage of the overall reflectance. This is done by determining the minimum reflectance between the two peaks on either side of the absorption band after the continuum has been removed.

4.3.3 Sample Origins, Chemistry and Spectra

To test the discrimination capability of spectroscopy for distinguishing indicator minerals a suite of indicator minerals from till samples collected over a known diamond occurrence is the data set used in this study. 106 pyrope garnets measured in this study, on loan from Diamonds North Resources Ltd, represent till samples collected from their Amaruk property in Nunavut in 2008 and supplemented with other known minerals from samples in the Brock University department collection. Mineral compositions for all of these grains were determined by electron microprobe analysis by Mineral Services Inc. Weight percents of the elemental analysis provided by this analysis have been converted to molecular proportions because individual cation substitutions may be better correlated to absorption depths by their molar fractions. Sample calculations have been provided in Appendix A.

These samples range from orange to deep purple in colour and in some cases were found to contain multiple small inclusions. Those samples with visible inclusions were removed to avoid any anomalous readings in the measured spectra. A mantle xenolith of unknown origin was used to determine the effect of various size fractions of pyrope with the same chemistry. Microprobe data for a few samples of this xenolith were obtained to confirm the consistency in chemistry for these grains.

4.4 Results

4.4.1 Cr Substitution in pyrope garnet

The chemistry of the garnets illustrates a negative relationship of Al_2O_3 and Cr_2O_3 (Figure 4.5). This confirms that there is Cr^{3+} substituting for Al^{3+} in the M2 crystallographic site. The trendline here indicates that there is a 1:1 relationship between these two elements suggesting that chromium substitutes preferentially into the M2 crystallographic site occupied by Al^{3+}.

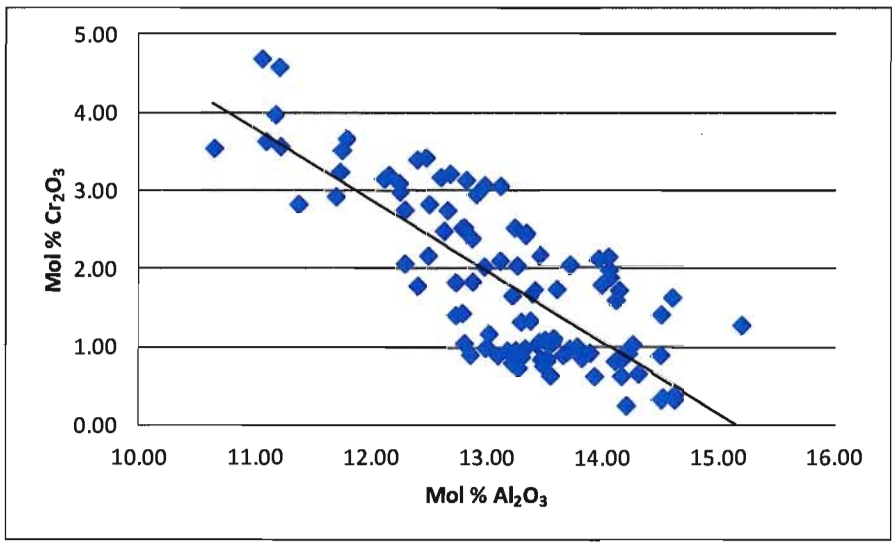

Figure 4.5: A sample size of 106 pyrope garnets illustrating the negative relationship in mol % of Cr^{3+} substituting for Al^{3+} in the M2 crystallographic site.

The Cr substitution relationship is spectrally illustrated in Figure 4.6 for two garnet grains, each similar in grain size (volume of 0.31 mm^3). The sample GP-08P-411 illustrates a well defined minor absorption feature at ~689 nm and is visible in the sample GP-08P-517 at ~ 0.5 times the magnitude of the first. This might be due to the low amount of chromium incorporated within the crystal lattice. Microprobe results indicate that the proportion of chromium in each sample is 6.84 and 4.39 mol % respectively.

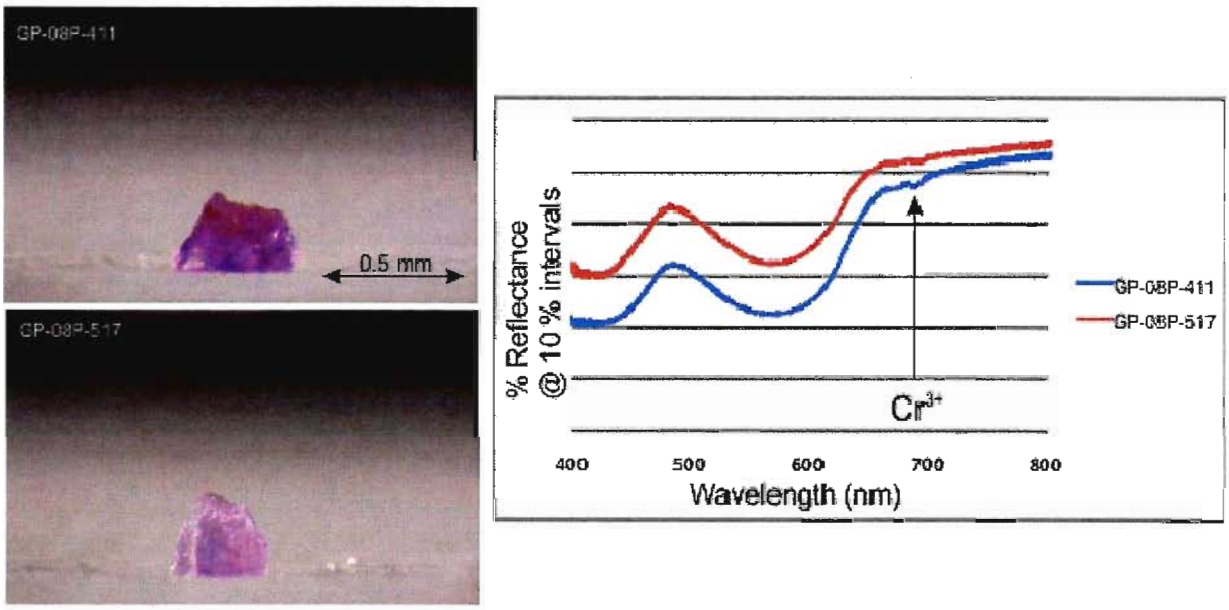

Figure 4.6: Graphs and images of two pyrope grains offset in % reflectance for clarity. These pyropes are similar in grain volume however at the wavelength of 689 nm garnet GP-08P-411 has a clearly defined absorption feature whereas garnet GP-08P-517 has a much smaller absorption feature, possibly by an order of magnitude. The Cr_2O_3 proportions are 6.84 and 4.39 mol % respectively.

The expression of the observed absorption band depth has a positive relationship with increasing Cr_2O_3. Although there is no spectral response associated with Al_2O_3 in the garnet mineral structure, because of the substitution relationship between Cr_2O_3 and

Al_2O_3, a negative relationship with Al_2O_3 content is expressed but is not causal since the absorption band depth plotted was chosen based on chromium (Figure 4.7).

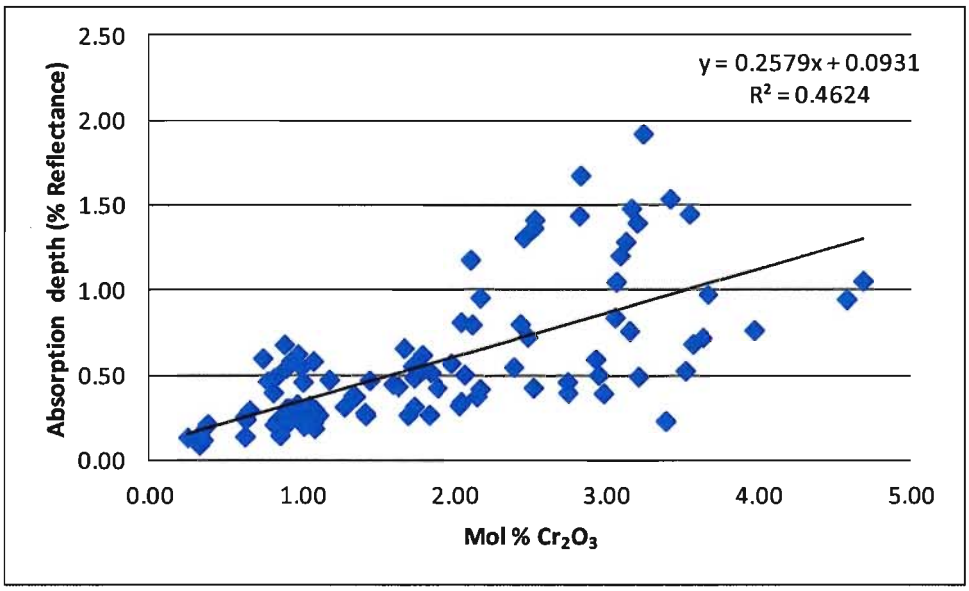

Figure 4.7: A graph of Cr_2O_3 vs the Absorption Band Depth at 689 nm for pyrope garnets illustrating the observation that as the proportion of Cr^{3+} increases the absorption band depth increases.

Figure 4.5 illustrates a strong relationship with respect to the proportion of Cr substituting for the Al in the M1 crystallographic site. Therefore the spectral reflectance characteristics in this particular site can be used to screen for high to low Cr content in pyrope garnet. This association is evident in all garnet grains even though the data has not been corrected for grain size.

4.4.2 Grain Size effect on pyrope garnets

A sample size of 30 garnets from a mantle xenolith source was measured to examine the relationship between grain volume (0.31 – 28.50 mm^3) and thickness (0.42 – 2.04 mm). This xenolith was found to contain chrome diopside, olivine altered to

serpentine and pyrope garnet. Pyrope garnets were sampled to produce a variety of grain sizes for spectral analysis. Four of these samples were randomly selected for microprobe analysis. The chromium content of these samples averaged 0.89 ± 0.09 mol %. Using the 30 samples of different grain size, thickness and volume measurements were made and spectral measurements of each were collected to determine depth of the Cr absorption band at 689 nm.

The correlation coefficient (Figure 4.8), for volume is greater than that for thickness. Therefore the absorption depth for the feature 689 nm has a more accurate relationship with grain volume than with thickness. Hence, grain volume will be used for grain size related relationships.

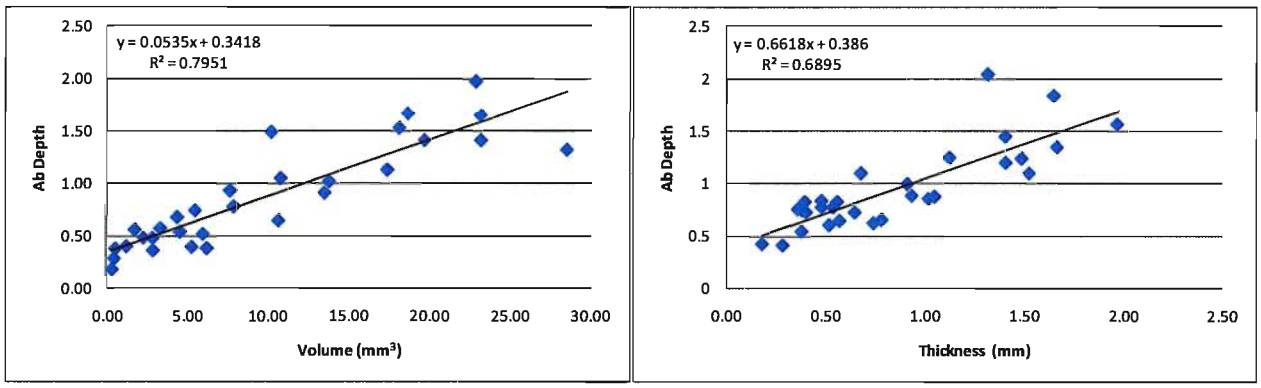

Figure 4.8: Thickness and volume plots vs absorption depth at 689 nm for 30 pyrope garnets from a mantle xenolith.

Figure 4.9 illustrates the range and variation in grain sizes of garnet from till samples provided by Diamonds North that were used in this study illustrating that the sample suite has a fairly continuous size distribution from 0.03 to 1.00 mm^3.

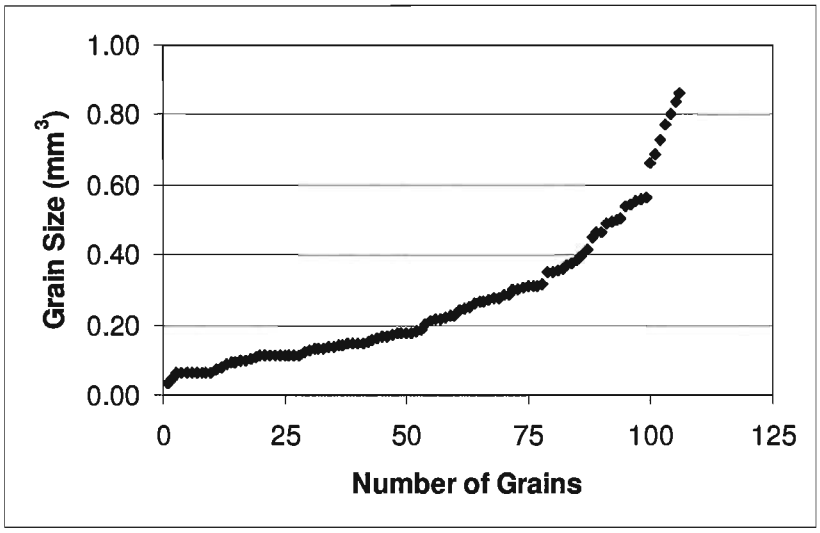

Figure 4.9: Grain volume distribution in the pyrope garnet sample population.

The spectrum of a particular grain will decrease in reflectance (effectively also deepening absorption bands) as grain size increases assuming the chromium content is the same. Figure 4.10 illustrates a very broad positive linear trend.

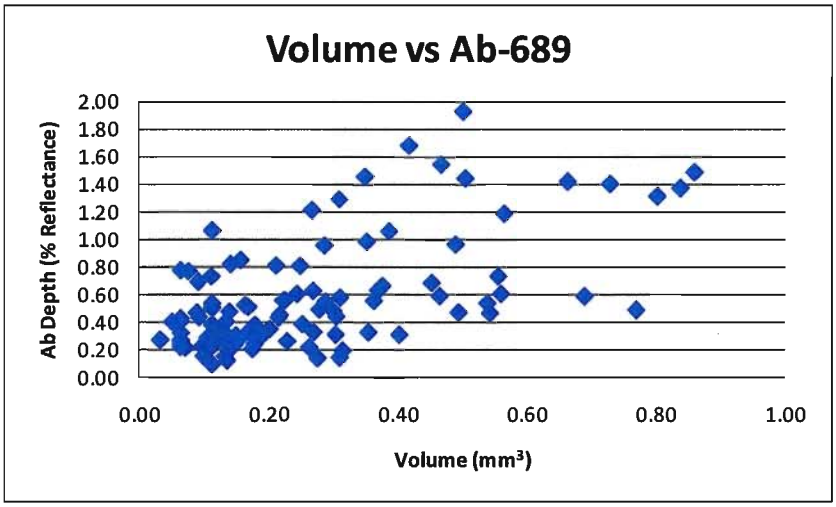

Figure 4.10: A scatter plot illustrating the relationship between Grain volume vs Absorption band for 106 pyrope garnets which have various grain sizes, ranging from 0.03 to 1 mm^3. The graph does not take into account the Cr content of the grains, which range from as little as 0.20 mol % to a maximum of 6.00 mol %.

To examine the effect of chromium content and grain size independently, grain fractions have been separated into six size categories. Figure 4.11a illustrates that the absorption depth for a given mol % Cr_2O_3 is higher for larger grains. However this relationship appears to saturate (with the laboratory apparatus used) once grain volume reaches about 0.4 mm^3. Different slopes exist for different grain size populations and the slope increases as the grain volume increases.

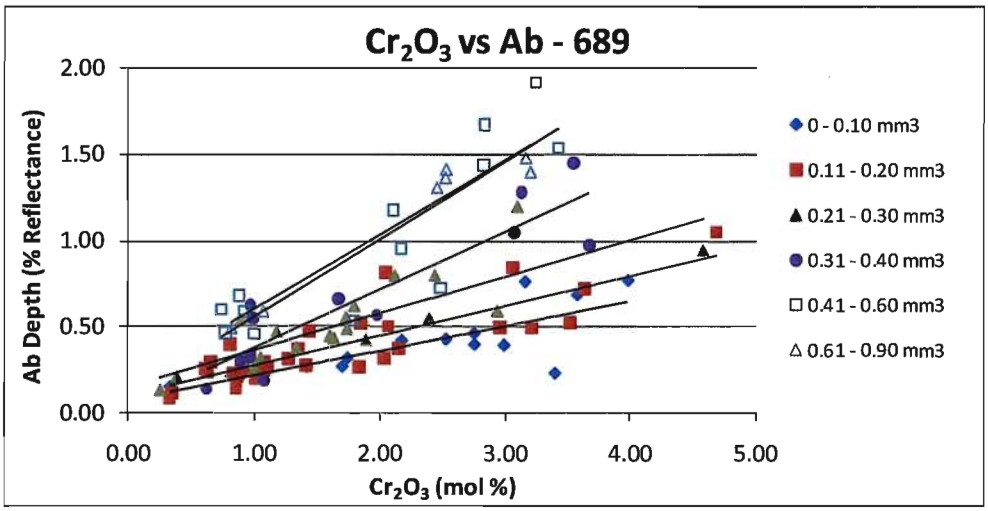

Figure 4.11a: Absorption band depth vs Cr_2O_3 proportion for various grain size fractions.

Separating the pyrope garnets into various grain size fractions (Figure 4.11b) helps to isolate the relationship between chrome content and absorption feature for each grain size fraction. Each grain size fraction shows a much improved linear relationship between absorption depth and molar chrome proportion. This indicates that the molar chrome content of a particular pyrope garnet grain can be estimated from the depth of this spectral absorption feature once grain volume is taken into account. In addition to some measurement uncertainty, we suggest that some of the remaining scatter could be

contributed by small inclusions or impurities within the garnets. A larger study with more samples and a wider range in chromium content would be required to further refine the relationship between chromium content and absorption feature depth for a given grain size.

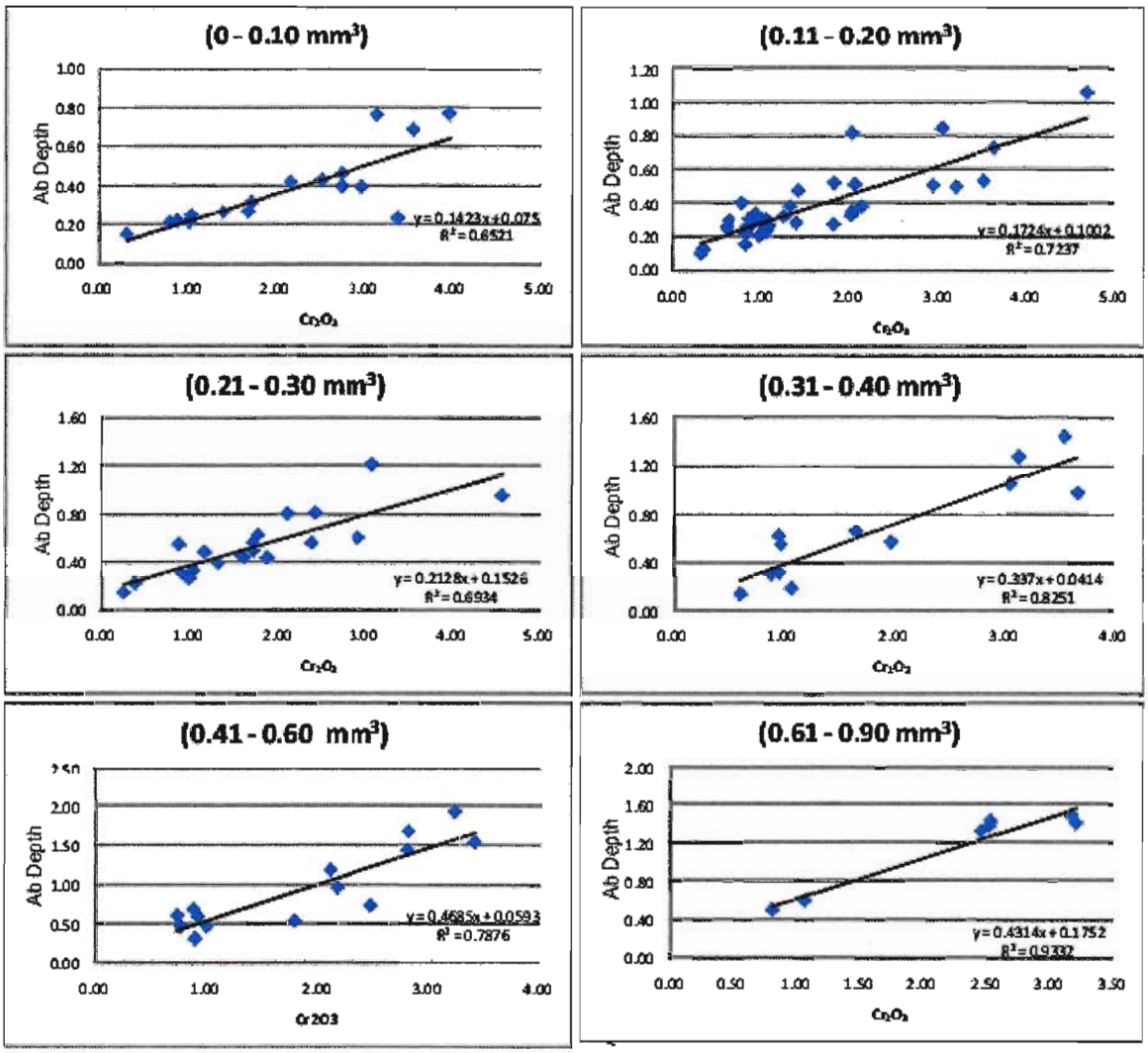

Figure 4.11b: Absorption band depth vs Cr_2O_3 proportion of pyrope garnets showing good linear relationships in separate graphs for various grain volume fractions.

4.5 Conclusion

The evidence outlined above indicates that the absorption feature at ~ 689 nm is due to substitutions of Cr^{3+} in a 6-fold symmetrically coordinated site in pyrope. The proposed unique Cr^{3+} absorption feature is visible and distinctive in minerals that have chrome quantities above 0.25 mol % included within the crystal lattice, which corresponds to 0.55 wt.%.

The methodology employed here suggests a cautious approach with measuring and taking images of each grain in 5 orientations to obtain accurate spectral data and visual observations, to reduce the average sampling noise and to investigate the relationships to geochemistry. This takes approximately 2 minutes total. However we observe in the data collected for 5 orientations, that reflectances are fairly similar due to the isotropic structure of garnet. For more rapid, operational applications, a single measurement from one orientation would make the process much faster and as reliable.

It is proposed that as visual inspection of till samples are made, taking spectral measurements of a few pyrope garnet grains may yield preliminary results of great interest. Once the volume and spectra have been measured the chromium concentration can be estimated using the graph and equations in Figure 4.11b. The method described is simple and the equipment required is portable and robust enough to function in field environments, requiring only a lap top computer and electrical power. Predictive estimates from samples taken in the field could help direct till sampling programs to improve the effectiveness of drift prospecting. The time it takes to obtain spectral measurements for many grains, prepare and send them for microprobe analysis is far less time than to get all grains mounted, microprobed and chemically analyzed.

Although the number of pyropes used in this study was limited, a good relationship between mol% Cr and absorption depth indicates that a predictive or semi-quantitative estimate of Cr content is possible using the spectral analytical methods. Additional spectra can be collected and processed to further improve the observed relationship and improve the results. It is evident that the method proposed in this study has demonstrated a successful, relatively rapid and effective approach for estimating the Cr content in pyrope garnets.

References

Burns, R. (1993) Mineralogical applications of crystal field theory: Crystal field spectra of transition metal ions in minerals. Cambridge topics in Mineral Physics and Chemistry. Cambridge University Press, New York. Pg. 1-190

Carstens, H (1973). The red-green change in chromium bearing garnets. Contributions to mineralogy and petrology. Vol. 41. Pg 273-276

Clark, R. N. (1999) Chapter 1: Spectroscopy of Rocks and Minerals, and Principles of Spectroscopy, in *Manual of Remote Sensing, Volume 3, Remote Sensing for the Earth Sciences*, (A.N. Rencz, ed.) John Wiley and Sons, New York, p 3- 58.

Clark, R., Hoefen, T., Swayze, G., Livo, E., Meeker, G., Sutley, S.,Wilson, S., Brownfield, I., Vance, S. (2003) Reflectance Spectroscopy as a rapid assessment tool for the detection of Amphiboles from the Libby, Montana Region *U.S. Geological Survey Open-File Report 03-128.*

Cloutis, E. (2002) Pyroxene reflectance spectra: Minor absorption bands and effects of elemental substitutions. J. Geophysical Research, 107: E6. Pg 1-12

Dawson, J.B., Stephens, W.E. (1976) Statistical Classifications of garnets from kimberlite and associated xenoliths. Addendum. J. Geol., Vol. 84, pg 495-496.

Deer, W.A., Howie, R.A., Zussmam, J. (1964) Rock Forming Minerals: Ortho- and Ring Silicates. Longman Group Limited, London. Pg 77-112.

Gurney, J.J., (1984). A correlation between Garnets and Diamonds in Kimberlite. In: Glover, J.E., Harris, P.G. (Eds.), Kimberlite occurrence and origins: A Basis for Conceptual Models in Exploration. Geology Department and University Extension, University of Western Australia, Publication 8. Pg 143 – 166.

Grütter, H., Gurney, J., Menzies, A., Winter, F. (2004). An updated classification scheme for mantle derived garnet, for use by diamond explorers. Lithos. Vol. 77. Pg 841-857.

Rost, F., Beermann, E., Amthauer, G. (1975) Chemical Investigation of pyrope garnet in the stockdale Kimberlite intrusion, Riley County, Kansas. American Mineralogist. Vol. 60. Pg 675 – 680.

Swayze, G.A., Smith, K.S., Clark, R.N., Sutley, S.J., Pearson, R.M., Vance, J.S., Hageman, P.L., Briggs, P.H., Meier, A.L., Singleton, M.J., and Roth, S., 2000, Using imaging spectroscopy to map acidic mine waste, Environmental Science and Technology, **34**. Pg. 47-54.

Van Ruitenbeek, F. J.A. Debba, P. Van der Meer, F.D. Cudahy, T. Van der Meijde, M.Hale, M. (2006) Mapping white micas and their absorption wavelengths using hyperspectral band ratios, Remote Sensing of Environment **102**. Pg. 211-222.

Chapter 5: Spectral characterization of some naturally occurring kimberlite indicator minerals using reflection analysis in the visible spectral region

5.1 Introduction

Spectral reflectance studies into some silicates (e.g. Cloutis et al. 1990, Rost et al. 1975) investigate the effects that major and minor transition metals within a mineral have on its reflectance spectrum. Such studies tend to be very specialized and can leave out minor absorption bands associated with elements bonded in particular minerals (Cloutis et al. 1990, Rost et al. 1975). Garnets for example have three end members in the pyralspite ternary system with end members based on the proportions of elements that occur in the M2 crystallographic site (Mg, Fe^{2+}, Mn) (Deer et al. 1964). However, minor substitutions of other elements into the M1 crystallographic site (Al, Cr^{3+}, Fe^{3+}, etc) (Deer et al. 1964) also occur within garnets and may be associated with minor absorption bands (Burns 1993). Pyrope garnet is the most common indicator mineral studied in kimberlite bodies because the amount of substituted chromium can be linked to the presence of diamond (Gurney 1984, Grütter et al. 2004).

Here we examine a number of minerals that share some of the same transition metal substitutions as pyrope. Minerals such as almandine, forsterite, diopside, chromite and ilmenite are examined as indicator minerals for the exploration of diamond bearing kimberlites. These minerals may form at the same time and in the same geochemical setting as pyrope garnet and can provide insights into the genesis of the kimberlite. For example, diopside can accommodate the Cr^{3+} ion into the M1 position of its molecular structure which is in the same octahedral coordination as pyrope garnet (Deer et al.

1964). The result of the similar lattice geometry is the location of the absorption feature in the reflection spectra of diopside at 689 nm, similar to that of pyrope garnet studied in Chapter 4.

We also examined the spectral properties of almandine, spessartine, grossular and ruby because they share molecular similarities with indicator minerals. Because the number of specimens studied here is not deemed large enough for a proper quantitative evaluation, the results of this study are primarily qualitative and intended to provide suggestions for further studies.

5.2 Mineral Origins and Descriptions

Primary samples for this study are on loan from till samples collected by Diamonds North Resources on their Amaruk property in Nunavut, Canada. Mineral samples picked and analyzed from these till samples include pyrope, almandine, forsterite, diopside, chromite and ilmenite. Other samples that were analyzed include spessartine, grossular, almandine from various sources, as well as pyrope and diopside from one single mantle xenolith. The source for these minerals varies from localities across Canada, most of which are unknown. The goal of using these minerals was to gain spectral data for kimberlite indicator minerals, mantle related minerals and several types of crustal garnets from various sources. Summary data for the minerals used in this study have been provided in Table 1 (Deer et al. 1964).

Table 1: Mineral Formulae, Grain Count and Origin.

Mineral	Molecular Formula	Grains analyzed	Origin
Pyrope	$Mg_3Al_2(SiO_4)_3$	106	Pelly Bay area, Nunavut and the Brock University collection
Almandine	$Fe^{2+}{}_3Al_2Si_3O_{12}$	30	Pelly Bay area, Nunavut and the Brock University collection
Grossular	$Ca_3Fe_2Si_3O_{12}$	28	Brock University collection
Spessartine	$Mn_3Fe_2Si_3O_{12}$	1	Pelly Bay area, Nunavut
Olivine	$(Mg, Fe)_2SiO_4$	43	Pelly Bay area, Nunavut
Diopside	$MgCaSi_2O_6$	9	Pelly Bay area, Nunavut and the Brock University collection
Chromite	$(Fe, Mg)Cr_2O_4$	10	Pelly Bay area, Nunavut
Ilmenite	$FeTiO_3$	10	Pelly Bay area, Nunavut
Ruby	Al_2O_3	5	Pelly Bay area, Nunavut

5.3 Method and Material

The experimental procedure used in this study follows the one outlined in Chapter 3 and sections 4.3.0 – 4.3.2 in Chapter 4. The setup and procedure has been previously proven to be quite accurate, quick and reliable. For this reason and to prevent repetition it will not be repeated here.

5.3.1 Sample Origins, Chemistry and Spectra

Mineral compositions for all mineral grains measured were determined by electron microprobe analysis by Mineral Services Inc. Following the procedure established in Chapter 3 & 4, weight percents of the elemental analysis have been converted to molecular proportions because individual cation substitutions may be better correlated to absorption depths by their molar fractions. As discussed below in Section

5.5, samples with visible inclusions were removed to avoid any anomalous readings in the measured spectra.

5.4 Results

5.4.1 Pyrope garnets

Pyrope garnet is the most abundant type of garnet found in kimberlite and is the most useful silicate mineral as an indicator of diamond occurrence. Several studies (Dawson and Stephens 1976, Gurney 1984, Grutter et al. 2004) have suggested that as the chromium to calcium ratio substituted into the pyrope molecular structure increases, the possibility of the kimberlite being an economic source of diamond increases. Chromium is a transition metal with an absorption band that is detectable in the visible spectrum of silicate minerals. This absorption band has been extensively studied and is dealt with in Chapter 4.

All types of garnet have small amounts of other elements, especially in the pyralspite group series garnets. Iron and manganese are found as small amounts in pyrope due to this solid solution series with almandine and spessartine (Deer et al. 1964). Other transition metal elements such as titanium, nickel or zinc can be found in these minerals but are in such trace amounts that they are either undetectable by spectral methods or are masked by larger absorption features. Correlations regarding the total iron proportions (FeO*) in Figure 5.1 indicate a negative relationship between FeO* and MgO and a weak positive relationship between FeO* and Al_2O_3. This suggests, without the aid of wet chemical analysis to quantitatively determine the ferric (Fe^{2+}) and ferrous

(Fe^{3+}) iron proportion that most of the total reported iron may exist as Fe^{2+} and only minor to trace quantities of Fe^{3+} are present.

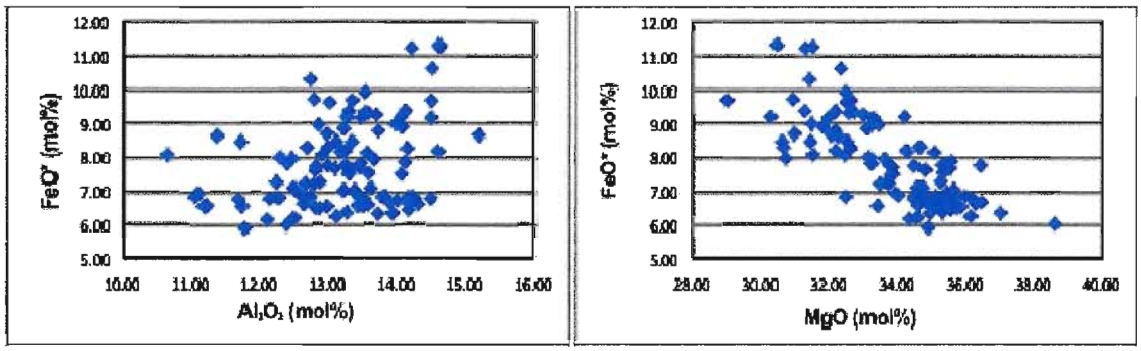

Figure 5.1: Two graphs that indicate a good 1:1 relationship of iron, primarily as Fe^{2+}, substituting for magnesium and not aluminum.

The proportion FeO in the pyrope garnet samples measured ranges from 5.94 – 11.33 mol % FeO. Over this wide range, the absorption features associated with the presence of Fe^{2+} in the visible region of the spectrum should be exhibited in the pyrope garnet spectra. Specific absorption bands in almandine garnet spectra are attributed in some studies to be the result of the proportion of FeO (Burns 1993, Manning 1967). These absorption features should be at the same wavelength in the pyrope garnet spectra if the cations are found in the same M2 crystallographic site and have the same molecular geometry as an almandine garnet. The reflectance spectra of pyrope and amandine garnet are illustrated in Figure 5.2. The goal of this was to attempt to correlate locations of Fe^{2+} absorption features in the pyrope spectrum relative to those already identified in previous studies (Burns 1993, Rost et al. 1975, Manning 1967).

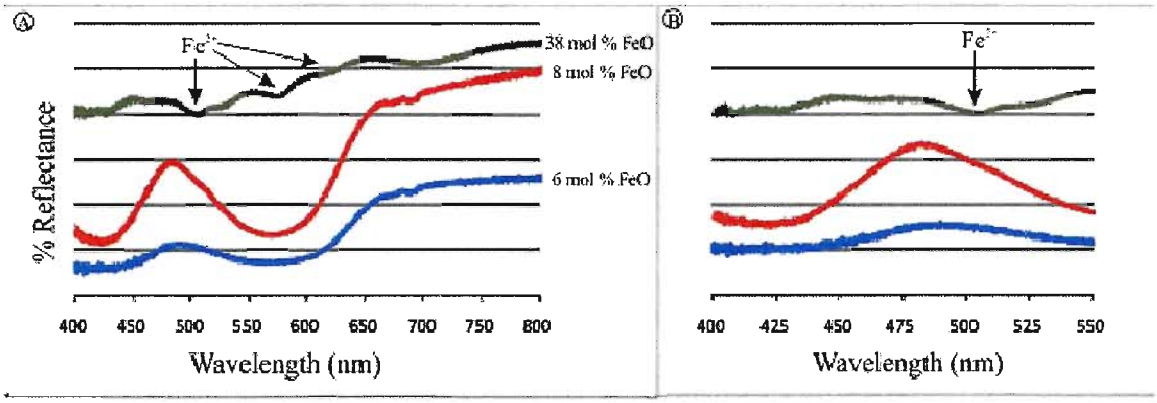

Figure 5.2: A: Reflectance spectra for 2 pyrope (red and blue) and 1 almandine (green) garnet grains showing the known locations of Fe^{2+} absorption features in the almandine spectrum (Manning 1967). B: Close up view of the absorption feature at ~505nm. Reflectance Spectra for each grain has been offset for clarity.

In Figure 5.2a locations for known absorption bands as identified by Manning (1967) are indicated on the plot of an almandine garnet with 38 mol % FeO. These absorption bands would be expected to be found at the same locations along the reflection spectrum of a pyrope garnet. The prominent absorption feature for chromium at 577 nm is broad and deep, making any other absorption feature near it irresolvable. A slight inflection at the side of this feature at ~505 nm could possibly be due to Fe^{2+} but a closer view of this is feature in Figure 5.2b makes it virtually invisible. Although Manning (1967) did report this feature in almandine being due to Fe^{2+}, the amount of FeO in pyrope (8 mol %) is not enough to detect in the spectral reflectance profile.

5.4.2 Almandine garnet

Almandine is the most common type of garnet due to its ability to form in igneous, metamorphic and sedimentary deposits. The spectra for three types of almandine from various locations are given in Figure 5.3 along with estimated transition metal absorption band centers and those given in literature (Burns 1993; Manning 1967).

Locations of Fe^{2+} absorption band centers are based on experimental and confirmed work however those for Mn^{2+} and Fe^{3+} are theorized having not been particularly significant in almandine or pyrope. The bands located at 410 nm and 500nm could be associated with the higher total Fe and Mn^{2+} content of these garnets as has been observed in similar silicate mineral investigations (Burns 1993). The association between the absorption features and the chemistry is still relatively uncertain. Further analysis through the calculation of absorption band depths in spessartine garnets of varying Mn^{2+} proportions and their relationships to grain volume and microprobe data may indicate some clearer relationship. However, the locations of these absorption bands are at very low reflectance levels and are very small suggesting that they may not be the only transition metal that is affecting the spectrum at this point.

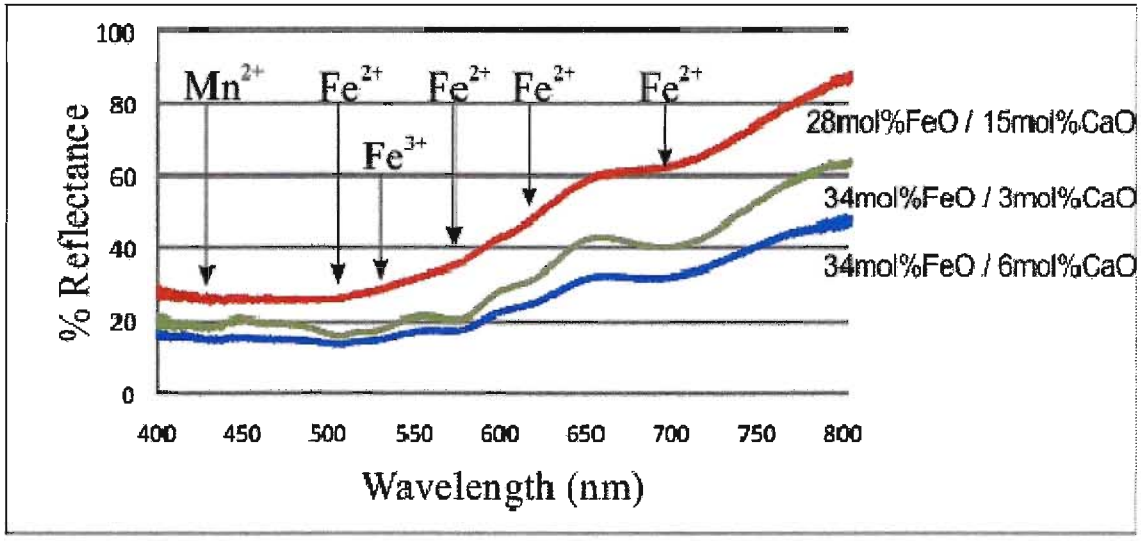

Figure 5.3: The typical reflected spectrum of 3 almandine garnets from different locations and environments. Red = eclogitic almandine, green = kimberlitic almandine, blue = crustal gneissic almandine. The position of absorption features that are labeled are those reported from Manning (1967) and this study.

Electron microprobe data acquired for the eclogitic and kimberlitic almandine samples suggests that the depth difference in absorption bands might be due to the inclusion of other elements into the crystal lattice of the eclogitic almandine samples. For example, the amount of FeO in eclogitic almandines varies between 27 – 30 mol % and the CaO between 14 – 16 mol % where as in the kimberlitic almandine samples the variation is between for 33 – 35 mol % FeO and 2 – 4 mol % CaO. This inclusion of other elements such as Ca^{2+} reduces the total amount of Fe^{2+}, which appears to result in the lower amplitude of associated absorption features. Minerals with more transition metal elements, such as Fe^{2+} in the kimberlitic almandine samples, have better developed absorption features at the absorption bands indicated in Figure 5.3.

5.4.3 Grossular garnet

This type of garnet was donated to Brock University by an unknown source and originally labeled as uvarovite. Uvarovite typically has an appreciable amount of chromium included within its crystal lattice. The mineral structure and crystallographic geometry is the same as pyrope but the composition is $Ca_3Cr_2Si_3O_{12}$. It has been analyzed to compare the similarities of it and Cr-pyrope. Microprobe results have confirmed the amount of Cr^{3+} included within this mineral is very similar to the quantities that exist in pyrope. However, due to the higher proportion of Fe_2O_3 that occupies the same crystallographic site these grains can be said to have more of a grossular type garnet component than uvarovite, thus is best described as a chrome-bearing grossular garnet. We can also expect a close resemblance of the absorption features related to the presence of Cr^{3+} in both grossular and pyrope garnets. Indeed, the spectral profile in Figure 5.4 of grossular is similar to that of pyrope due to the large proportion of Cr^{3+} in both, however

the spectrum of the chrome-bearing grossular garnet seems to be shifted by ~ 35 nm to higher wavelengths. The absorption band typical for Cr^{3+} is visible at ~700 nm, although when the continuum is removed, it is found at the same location as pyrope, approximately 689 nm.

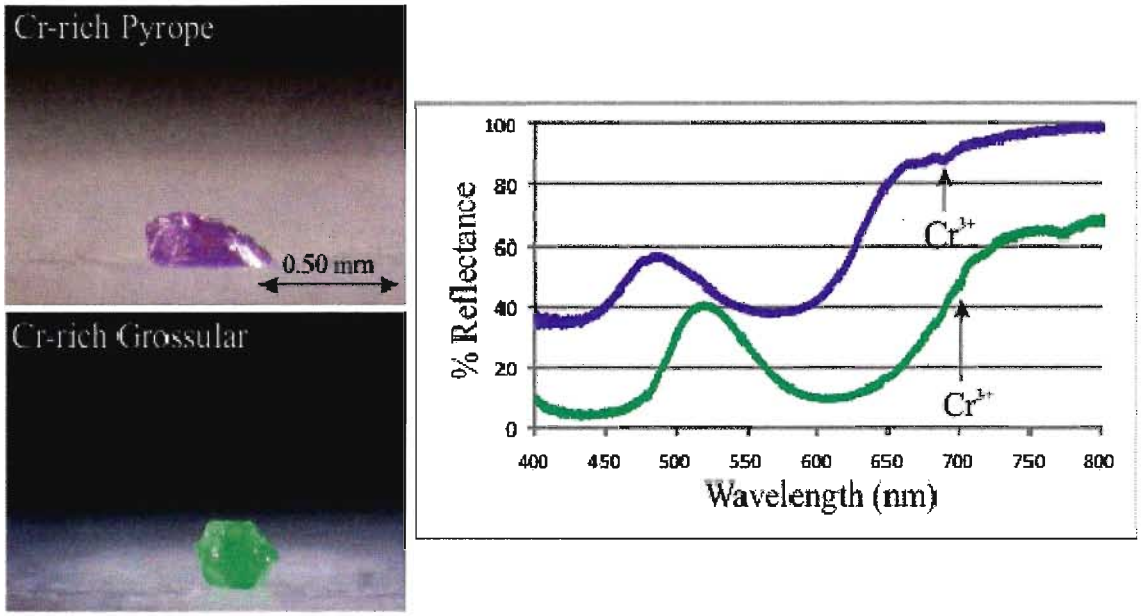

Figure 5.4: The spectral graphs for pyrope and grossular garnets indicating the similar spectra and the shifts in Cr^{3+} absorption band locations.

This observation suggests that chromium, when included in the crystal lattice of a garnet structure can be indicated by a minor absorption feature at ~689 nm. Once the continuum on the slope of the reflectance spectra has been removed the absorption band is at the same location in both garnet varieties. The overall shift in spectra could be due to large variations in the mineral chemistry. One large variation in the microprobe data is the proportion of magnesium in the pyrope, diopside and grossular. Pyrope and diopside both range from 29 – 39 mol % MgO whereas the MgO proportion in grossular has been completely replaced by CaO. Another difference in the compositions is the CaO

proportion. In pyrope it ranges from 2 – 9 mol % and in diopside from 16 – 27 mol %. The CaO proportion in grossular accounts for ~ 40-50 mol % of the chemical composition which may have an effect on the absorption band locations, their depths and possibly shifts towards the red part of the spectrum. This relationship remains unclear and requires additional data to fully investigate the role of CaO and MgO on the spectral properties.

5.4.4 Spessartine garnet

This type of garnet is the Mn^{2+} endmember of the solid solution between pyrope (Mg^{2+}) and almandine (Fe^{2+}). Although only one sample of spessartine was obtained through this study, samples of almandine and pyrope which contain quantities of manganese can be used to qualitatively correlate and match to absorption features already identified by Manning (1967) (Figure 5.5).

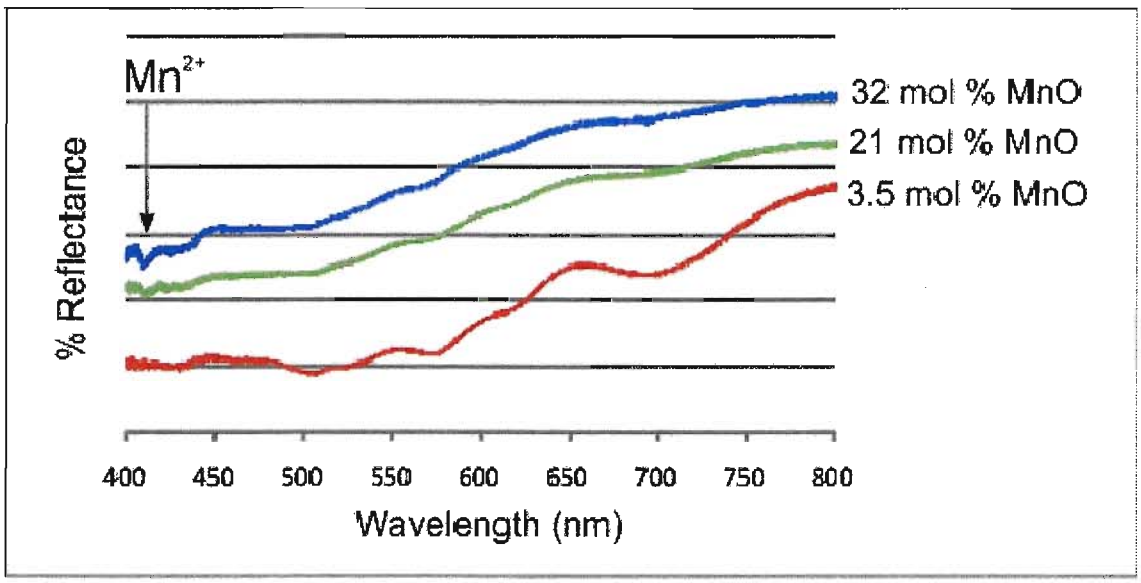

Figure 5.5: Spectral graph of 1 spessartine grain (blue) and two almandine grains with a large difference in MnO proportions (green, red).

The location of the Mn^{2+} absorption feature in spessartine is identified in Figure 5.5 as a narrow absorption feature at ~405 nm (blue). This feature can also be identified in the spectrum of the almandine with a large proportion of MnO (green). This feature decreases in magnitude as the proportion of MnO decreases from 32 mol % to 21 mol% in this almandine. The feature becomes unidentifiable in the almandine spectrum (red) with a low proportion of only 3.5 mol% MnO.

5.4.5 Olivine - Forsterite

Forsterite to fayalite series olivines are known to occur in many types of igneous and metamorphic rocks, meteorites and lunar basalts and have been the subject of spectroscopic studies (Cloutis 2002, Burns 1993). Forsteritic olivine tends to be the most common mineral in kimberlite bodies due to its high availability as a mantle related mineral. Of particular interest to this study is the evidence that olivine has site preferences for various transition metal elements including Fe^{2+}, Mn^{2+} and Ni^{2+} (Burns 1993). Varieties of olivine that form in mantle conditions will be composed of primarily Mg_2SiO_2 with traces of other elements that substitute for magnesium. These substituting elements are mostly transition metals. As typical of most transition metals, these elements will result in characteristic absorption bands in the reflectance spectra.

The typical range of five forsterite reflectance spectra taken from the 43 samples measured is given in Figure 5.6 to indicate the variation in the absorption features as the molecular proportion of transition metal geochemistry changes.

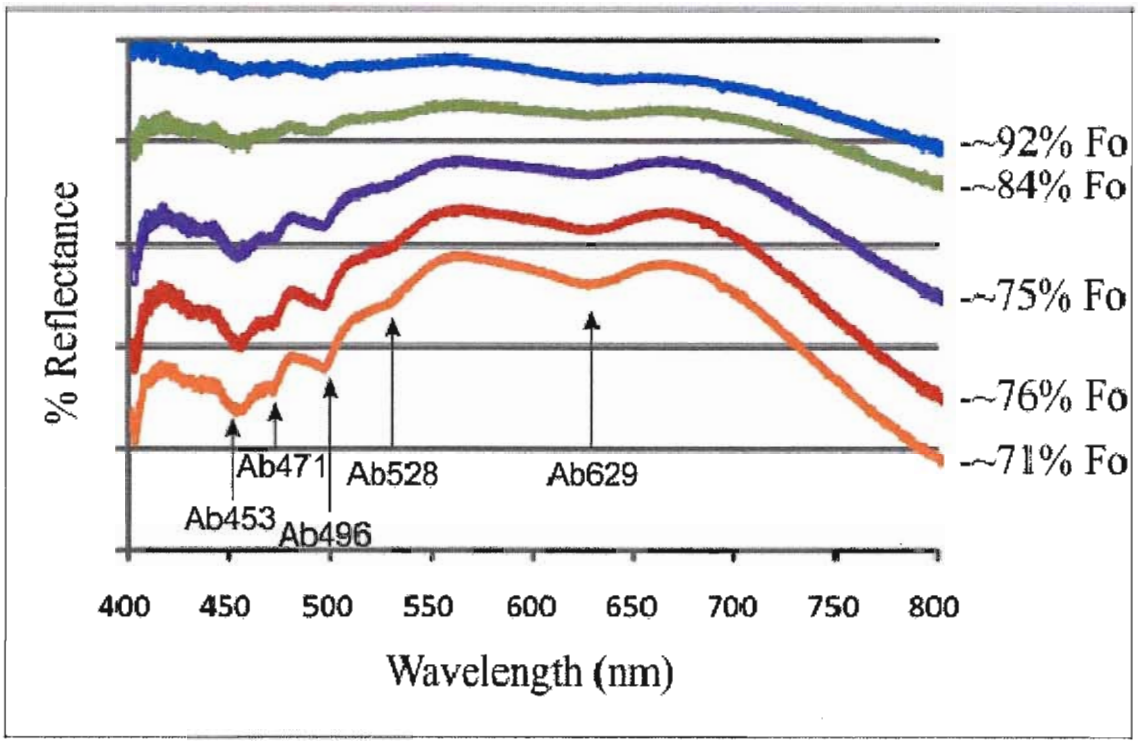

Figure 5.6: Typical reflectance spectrum of 6 various forsteritic olivine grains. The general trend of the change in absorption band magnitude is the increasing proportion of MgO and the decreasing proportion of FeO*. Reflectance Spectra for each grain has been offset for clarity.

The reflectance spectra given in Figure 5.6 for six forsteritic olivine grains exhibits many absorption bands in the visible region. In Figure 5.6, the sample in orange has 20 mol % FeO and the blue sample has 5% FeO with all other samples in between. Furthermore, the depth profiles of each absorption band increase collectively. The trend that can be observed in the spectral reflectance plots is a flattening or decrease in absorption bands as the proportion of FeO* decreases and the proportion of MgO increases. This relationship is not evident when graphing the depths of various individual or packaged absorption features versus transition metals.

5.4.6 Diopside

These samples have been subdivided into two categories: chrome diopside (>0.50 mol % Cr_2O_3) and low-chrome diopside (<0.50 mol % Cr_2O_3). The high quantity of chromium occurring in this mineral has been suggested to be associated with diamondiferous kimberlites similar to the chrome-bearing G10 pyrope garnets. In Figure 5.7 two images of diopside and their corresponding reflectance spectra illustrate the presence and absence of the Cr^{3+} absorption band. This feature is visible in roughly the same position (~689 nm) for similar silicate minerals, such as the pyrope garnets described in the previous Chapter. Although this absorption feature is absent in the low-chrome diopside sample, microprobe analysis has confirmed the presence of Cr_2O_3 < 0.14 mol % which might not be a sufficient quantity to cause a recognizable absorption band with our apparatus used.

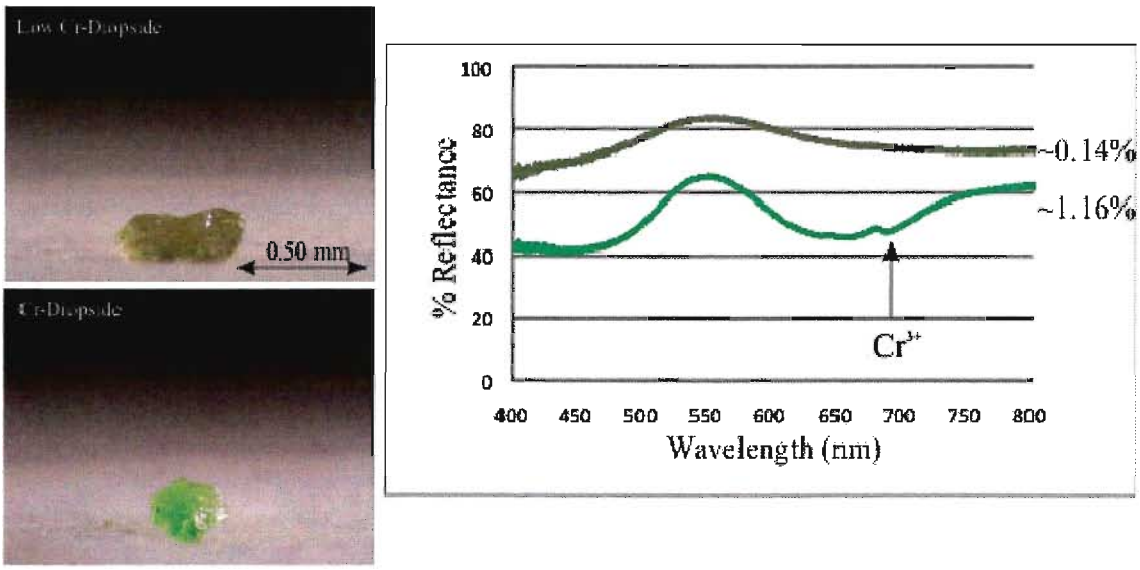

Figure 5.7: Images and their corresponding spectral graph of two diopside grains illustrating the presence/ absence of the Cr^{3+} absorption feature typically seen in pyrope garnet. Also note the colour of the two grains. Diopside with Cr^{3+} proportions over 1 mol % will appear lime green where as lower proportions will appear a dull olive green.

The molecular formula for diopside is $CaMgSi_2O_6$ where the X site (Ca) is typically substituted with divalent and smaller cations in distorted 6-fold coordination and the Y site (Mg) is substituted with divalent, trivalent and larger cations (Burns 1993). Chromium cations found in the Y site are attributed to the same absorption band in chrome pyrope due to being in the same crystallographic symmetry (6-fold coordination). The absorption band being produced is a direct result of the energy difference in the d-orbitals. This is why it is possible for Cr^{3+} to have similar absorption band wavelengths for pyrope garnet and chrome diopside. This feature is also thought to occur in minerals where Cr^{3+} is at least a minor component and is in 6-fold (octahedral) coordination with its surrounding ligands.

Grains came in 2 distinct size ranges five which are clustered between 0.08 – 0.29 mm^3 and four clustered between 0.98 – 3.03mm^3. Relationships between grain volume and absorption band depths are outlined in Chapter 4 for pyrope garnets. This relationship is also thought to occur with chrome-rich diopside as suggested in Figure 5.8.

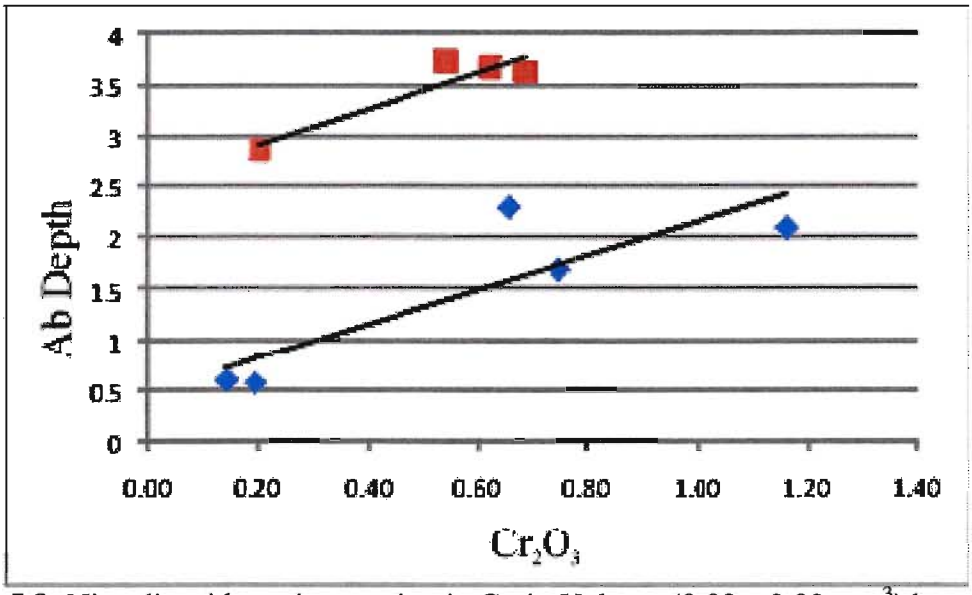

Figure 5.8: Nine diopside grains varying in Grain Volume (0.08 – 3.03 mm^3) here with absorption band depth plotted against Cr_2O_3 proportions. Grains that are relatively close in grain volume fractions show a linear relationship as indicated by the volume fraction for 0.08 – 0.29 mm^3 in blue. This relationship also exists as grain volume and volume fractions increase in size as indicated by the size fraction 0.98 – 3.03 mm^3 in red.

This grain size association is clear in each grain size fraction as Cr_2O_3 and absorption depth increase. Limitations to this correlation are the limited number of samples and the low reflectance percentage in the spectrum.

5.4.7 Oxides – Chromite and Ilmenite

Ilmenite and chromite both contain transition metal elements and are found abundantly in kimberlite as indicator minerals. However, the high absorption across the visible range measured, in the range of 2 to 6% typically, and opacity of each do not allow reflected light to reveal any absorption features and thus for these reasons, no indication of the transition metal content is evident. As observed in Figure 5.9, the reflected spectrum of these oxide minerals is given as a straight line in the visible spectrum.

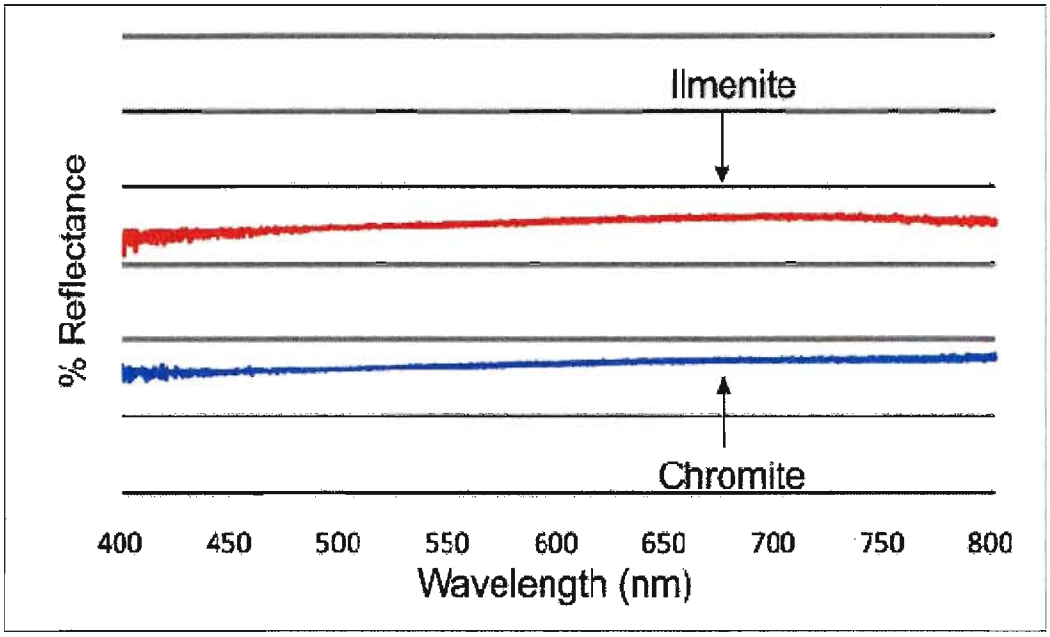

Figure 5.9: Spectral graph of both a chromite grain and an ilmenite grain. No distinctive absorption bands are diagnostic in this region. Vertical axis is set at 10 % intervals and spectra are offset for clarity.

5.4.8 Ruby

In the same way that absorption bands indicate the presence of specific transition metal elements, emission bands can indicate the same element provided that element is in the same coordination symmetry (Figure 5.10). Ruby is a type of corundum that has roughly 1% Cr^{3+} substituting for Al^{3+} in distorted octahedral coordination (Nassau 1978).

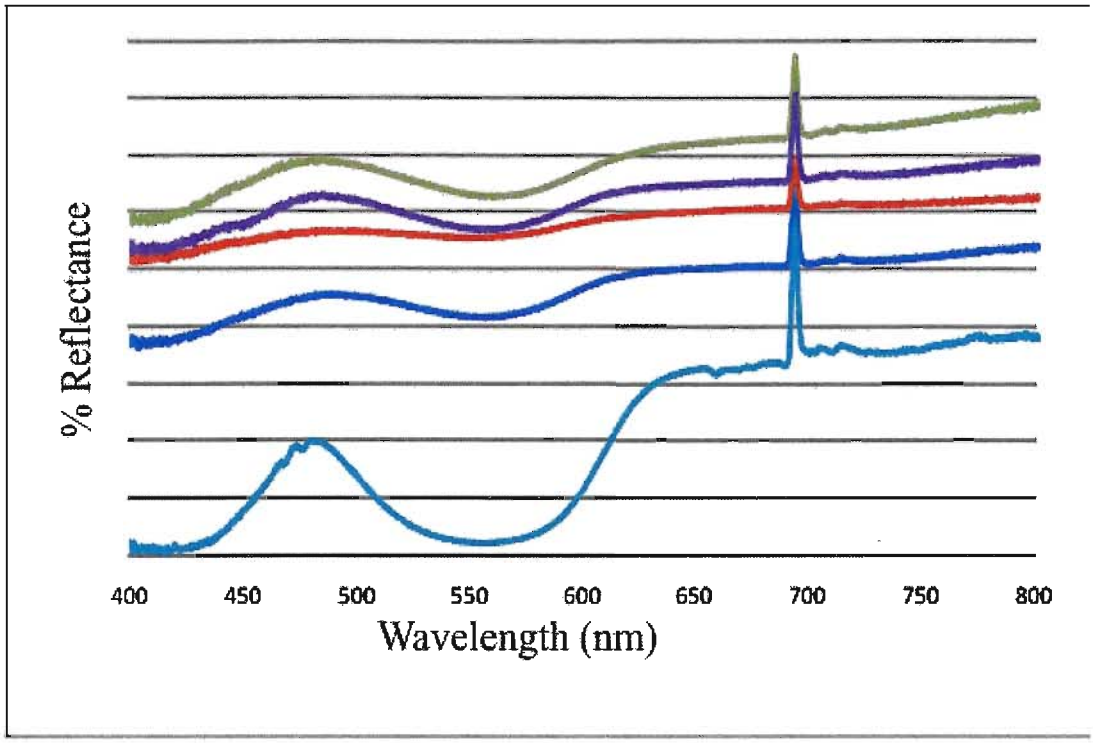

Figure 5.10: The reflectance spectra of various samples of ruby corundum.

The spectral reflectances reveal similar absorption in green and yellow light (near 550 nm) between pyrope and ruby and high reflectance in red light (near 650 nm) except for a unique emission peak at the same point (Figure 5.10) in the ruby spectra as the absorption band used to correlate to mol percent in pyrope (Chapter 4). This emission peak is also the same wavelength as that used in red lasers (i.e., 689 nm). The measured position of this emission peak at 689 nm is independent validation that the calibration of the Ocean Optics USB4400 spectrometer used in our apparatus set up is correct.

5.5 Sources for Error

Anomalous readings in spectral data may arise from various mineral and opaque inclusions that naturally occur within or on the surface of mineral grains. In many of the samples studied very fine grained inclusions occur which may not have a significant

outcome on the spectral data collected. However, some grains have been identified to include relatively large opaque minerals that may occupy a large portion of the actual grain volume (Figure 5.11).

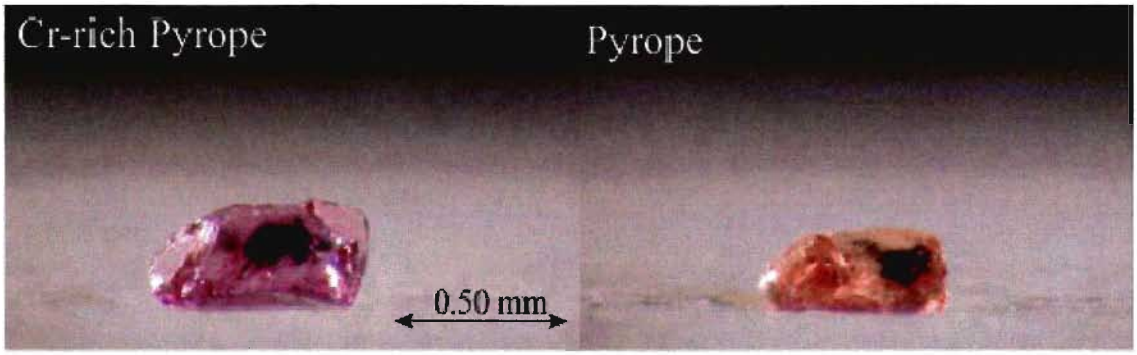

Figure 5.11: Cr-rich Pyrope garnet (left) and pyrope garnet (right) with large opaque inclusions.

Opaque minerals are known to absorb light at all wavelengths in the visible spectral region. This could have a significant effect on the overall outcome of the reflected light collected from an affected sample. Similarly very fine grained inclusions in a mineral may not have the same effect on the reflected light but could give unwanted results in the microprobe data. In kimberlitic indicator minerals the most common opaque inclusion is chromite. If part of this mineral was sampled with pyrope garnet the result would have a much different spectrum possibly visible as an opaque mineral. This would make it difficult to quantify the proportion of chromium and result in the incorrect identification of possibly a G10 garnet instead of a G0 or G1. The grossular sample set also shows inclusions as well as unwanted mineral associations that may affect the data collected. The digital camera provides a magnified view of the grain which enables the operator to immediately decide if the grain is suitable for measurement by preferentially picking out grains that do not hold inclusions.

5.6 Conclusion

The spectral absorption features of indicator minerals measured in this study have been examined in comparison to their mineral chemistry. This study primarily focused on various types of garnet but other kimberlite indicator minerals such as diopside have also been investigated to determine if the chromium absorption feature could be studied in the same method as it was in Chapter 4.

The absorption feature at 689 nm is identified at the same wavelength location as that for the chromium in pyrope garnet however scattering of data is still observed to be a problem. Grain size was used in the same method as in Chapter 4 to determine any relationship between chromium and the depth of this absorption feature. Clustering the data into grain size fractions seems to resolve the scattering of the data into linear trendlines for each cluster group. Although a trend is visible and the linear relationship is identified in two grain size fractions, limitations still exist in the lack of a large sample set. The value of this observation is that it confirms that certain size fractions should be chosen when using metrics such as depth of the spectral absorption features, to predict mineral chemistry or mol % of a particular cation.

Although pyrope garnet has been discussed in Chapter 4, this report attempted to provide additional information to help resolve features in the spectrum that may have been due to Fe^{2+}. A slight feature is visible along the side of the large absorption feature at ~ 505 nm. However, values cannot be resolved when attempting to calculate the intensity of this feature. This is due to the amplitude of the absorption feature and the effect of the proximity of the chromium absorption feature at 577nm. This large

absorption feature is also responsible in the pyrope spectrum for concealing the two other Fe^{2+} absorption features typically visible in the almandine spectrum and identified by Manning (1967).

Each absorption feature in the visible spectral region of the spectrum of almandine has been attributed to specific transition metal elements as illustrated in Figure 5.3. Using a variety of types of almandine it has been possible to determine the effect that differences in transition metal and non-transition metal geochemistry will have on a specific almandine grains reflected spectrum. Increases in the minerals calcium content decreases the amplitude of FeO* absorption features and vice versa. In other words, kimberlitic almandine grains with more mol % FeO and less mol % calcium will produce more defined absorption bands.

The absorption features that are distinctive of spessartine have been investigated by Manning (1967) however the depth relationship of these absorption bands with variations in geochemistry or grain size have not been examined. As proportions of manganese increase, the narrow characteristic feature at 405 nm is suggested to increase in depth as a result. This feature is visible in garnets that have more than 10 – 15 mol % substituting MnO, it is below this value that the feature becomes irresolvable. Although it is possible to determine these differences by visual interpretations there are not enough spessartine grains in this study to make any definitive conclusions.

The relationships between the absorption features for grossular garnet located at 689 nm are also associated with the Cr_2O_3 proportion. However, the connection between grain volume and absorption band depth is uncertain. These factors do not show a

positive relationship as determined for pyrope and diopside. It is proposed here that this is due to depth and temperature of formation. Microprobe data suggests that these garnets contain more of a grossular composition and a lesser uvarovite composition. These bright green grossular garnets could possibly be associated with a hydrothermal ore deposit such as those found in skarns. However this is just speculation due to the sample location remaining unknown. If this is the case these garnets were formed at low pressures and moderately high temperatures. In contrast, the pyrope garnets and diopside grains were formed at mantle conditions in extremely high temperatures and pressures. This difference would cause the crystal structure of the pyrope and diopside to be more closely packed with limited internal defects whereas the grossular may have a high concentration of internal defects and structural dislocations. These crystal abnormalities have been determined to have an effect on the visible reflected spectra from various grains in addition to an effect on the colour of the grain (Nassau 1976).

The spectrum of forsteritic olivines tends to illustrate more absorption features as their mol % of Fe^{2+} content increases. An examination of various graphs of transition metals versus absorption depth has suggested that more parameters must be involved in this relationship and further study is needed. The spectral graphs also indicate that as the mol % of MgO increases the slope of the spectra, and the amplitude of the absorption features decrease. Although this observation is not quantifiable in the limited sample set available it still suggests the proportion of MgO relative to FeO or transition metal content.

Preliminary findings of these spectral measurements are promising and indicate that there is an association of mineral chemistry to identifiable spectral properties, however in order to elucidate the quantitative relationships that were recognized for pyrope garnet indicator minerals in the previous Chapter will require a larger sample set.

References

Burns, R. (1993) Mineralogical applications of crystal field theory: Crystal field spectra of transition metal ions in minerals. Cambridge topics in Mineral Physics and Chemistry. Cambridge University Press, New York. Pg 1-190.

Cloutis, E. (2002) Pyroxene reflectance spectra: Minor absorption bands and effects of elemental substitutions. Journal of Geophysical Research, 107: E6. Pg 1-12

Cloutis, E., Gaffey, M., Smith, D., Lambert, R. (1990) Metal Silicate Mixtures: Spectral properties and applications to Asteroid Taxonomy. Journal of Geophysical Research, Vol. 95; No. B6: Pg 8323-8338.

Dawson, J.B., Stephens, W.E. (1976) Statistical Classifications of garnets from kimberlite and associated xenoliths. Addendum. J. Geol., Vol. 84: Pg 495-496.

Deer, W.A., Howie, R.A., Zussmam, J. (1967) Rock Forming Minerals: Ortho- and Ring Silicates. Longman Group Limited, London. Pg 77-112.

Gurney, J.J., (1984). A correlation between Garnets and Diamonds in Kimberlite. In: Glover, J.E., Harris, P.G. (Eds.), Kimberlite occurrence and origins: A Basis for Conceptual Models in Exploration. Geology Department and University Extension, University of Western Australia, Publication 8. Pg 143 – 166.

Grütter, H., Gurney, J., Menzies, A., Winter, F. (2004). An updated classification scheme for mantle derived garnet, for use by diamond explorers. Lithos. Vol. 77: 841-857.

Manning. P.G. (1967) The optical absorption spectra of the garnets almandine, pyrope and spessartine and some structural interpretations of mineralogical significance. Canadian Mineralogist. Vol 9. Pg 237- 251

Nassau, K. (1978) The origins of colour in minerals. American Mineralogist. Vol. 63. Pg 219 - 229.

Rost, F., Beermann, E., Amthauer, G. (1975) Chemical Investigation of pyrope garnet in the stockdale Kimberlite intrusion, Riley County, Kansas. American Mineralogist. Vol. 60. Pg 675 – 680.

Chapter 6: Conclusion

Reflectance spectra have been used in the past to identify specific minerals by recognizing particularly diagnostic absorption features present (Burns 1993). Many of these absorption features have been successfully correlated with the occurrence of various first series transition metal elements (Manning 1967, Rost et al. 1975). These elements have become recognized as the cause of such absorption features due to their presence within crystal fields created by atomic orbital interactions with various geometric orientations of ligands (Burns 1993). In the past these features have been used to predict the presence of these elements. The primary goal of this study was an attempt to relate the proportion of a transition metal to the depth of an absorption feature. Particular focus was on mantle related minerals recovered from drift prospecting samples and kimberlite to potentially use the results as a tool in discriminating diamondiferous from non-diamondiferous kimberlite occurrences. These mantle related minerals collectively called indicator minerals reflect the chemistry and transition metal content of their origin. These indicator minerals, when found in association with diamond in kimberlite pipes, will have high proportions of chromium (Gurney 1984). Several absorption features are seen along the spectra of indicator minerals indicating the presence of various transition metals. Pyrope garnet for example has three features in the visible spectral region all attributed to the presence of chromium. Two of these features are very broad and may overlap with other absorption bands associated with other transition metal elements. The other absorption feature is located at 689 nm and can indicate the chromium mol % with reasonable accuracy. This feature is advantageous to use because it occurs in part of the spectra that has a somewhat high percentage of

reflectance and the absorption band is not associated or near other metal absorption features in the pyrope spectra.

The chromium absorption feature is visible and distinctive in pyrope garnet that have quantities above 0.25 mol % (0.55 wt. %) included within the crystal lattice. After a volume and spectral measurement are taken, spectral data is processed using the experimental procedure from Chapters 3 & 4. Once the continuum is removed from the spectra the depths of absorption features are calculated and correlated with the chromium mol %. As the Beers-Lambert law states, the amount of light being absorbed is proportional to the number of absorbing elements that the light passes through (Burns 1993). This principle is usually taken into account using a measurement of thickness. Sample grains used in this study are not large enough to fill the field of view that is being sampled by the fiber optic cable. To account for the variation in the surface reflections and internal photon absorptions of grains from small to large sizes, the volumes of these grains are calculated and clustered into fractions. Absorption depth measurements and grain volume measurements has been successful in estimating the proportion of chromium in a particular pyrope garnet using the graphs in Figure 4.11b from Chapter 4. The data that is collected using absorption depth and grain volume to determine the chromium mol % is meant to be used as a preliminary test and can be integrated with standard identification and research practices typically used in the laboratory or in the field. This data can be collected prior to sending away mineral grains to determine exact chemistry by electron microprobe analysis.

The absorption feature located at 689 nm and correlated to chromium proportion in pyrope garnets is also evident in other indicator minerals such as diopside. Since the chromium ion in both cases is trivalent and in the same octahedral geometry, it is expected to have similar features in the reflectance spectrum. The same method outlined in Chapter 4, correlating absorption feature depth with mol % chromium, was used for diopside grains in two close volume fractions. Although a seemingly linear relationship is identified in two grain size fractions which correlate the depth of absorption to the proportion of chromium, the results have limitations due to the small sample set.

This study used a conservative approach with measuring and taking images of each grain in 5 orientations to obtain accurate spectral data and visual observations, to reduce the average sampling noise which takes approximately 2 minutes total. For more rapid, operational applications, a single measurement from one orientation would make the process much faster and statistically just as reliable.

The contribution of this experimental application and procedure to exploration geology could assist in other deposit types in addition to kimberlites. Skarn deposits for example have been mined for a variety of metals including Fe, W,Cu, Pb, Zn, Mo, Au, U, REE and Sn (Meinert et al. 2005). Defined by its mineralogy, skarn is dominated by calc-silicate minerals such as garnet and pyroxene. These rock types have a general zonation pattern of garnet and distal pyroxene which may exhibit systematic compositional and colour variations within the pattern (Meinert et al. 2005). Proximal garnet is commonly dark red-brown (Fe-rich) which becomes lighter brown to pale green further away from the source (Fe-poor). Pyroxene shares a similar but less evident

change in colour however it seems to increase in Fe or Mn further away from the source (Meinert et al. 2005). Compositional variations have been proven to be detectable in the reflected spectrum of garnet and pyroxene and in some cases these compositions are quantifiable. Of course a great deal of study is needed to determine if the proximity to a skarn deposit or possibly the economic viability of the deposit can be correlated to reflectance spectra of the indicator minerals as it does for some kimberlite indicator minerals.

References

Burns, R. (1993) Mineralogical applications of crystal field theory: Crystal field spectra of transition metal ions in minerals. Cambridge topics in Mineral Physics and Chemistry. Cambridge University Press, New York. Pg. 1-190

Gurney, J.J., (1984). A correlation between Garnets and Diamonds in Kimberlite. In: Glover, J.E., Harris, P.G. (Eds.), Kimberlite occurrence and origins: A Basis for Conceptual Models in Exploration. Geology Department and University Extension, University of Western Australia, Publication 8. Pg 143 – 166.

Manning. P.G. (1967) The optical absorption spectra of the garnets almandine, pyrope and spessartine and some structural interpretations of mineralogical significance. Canadian Mineralogist. Vol 9. Pg 237- 251

Meinert, L.D., Dipple, G.M., Nicolescu, S. (2005) World Skarn Deposits. Economic Geology 100th Anniversary Volume Pg 299-336

Rost, F., Beermann, E., Amthauer, G. (1975) Chemical Investigation of pyrope garnet in the stockdale Kimberlite intrusion, Riley County, Kansas. American Mineralogist. Vol. 60. Pg 675 – 680.

Appendix

A digital appendix has been attached to this thesis containing relevant mineral data. This includes original reflectance spectra and pictures of all minerals in Appendix A. Data that has been calculated and processed to determine the depths of specific absorption features following the removal of the continuum and artifact features can be found in Appendix B. Appendix C contains the mineral chemistry as received from Mineral Services Inc. As mentioned in the methodology the fiber optic cable and reference panels were subjected to tests to determine the most suitable equipment for this study. The data for these tests are provided in Appendix D. Appendix E contains calculations for conversion from wt % to mol % and all correlations between absorption depth, grain size and mineral chemistry.